



---

## Based on the Space-Time of String Theory Exploring Dark Matter Inside the Earth

Hsien-Jung Ho

Host / Newidea Research Center, Address: 10 Floor, No. 110-6, Jie-Shou N Road, Changhua City, Taiwan, R.O.C.; email: [newidea.ufoho@msa.hinet.net](mailto:newidea.ufoho@msa.hinet.net)

---

**Abstract** Applying the String theory, ten-dimensional space-time theory, to solve the scientific problems. According to “Causality Principle” and “Anthropic Principle”, the full Universe may be divided into triple Universes, and the dark matter should be taken as a terrestrial planet in other space than ours. The best method of exploring dark matter is to start from the Earth. According to the characteristics of the Earth's interior, equitably examining its constitution, temperature, density and pressure from a different view of the core, then the special arguments are put forward. The great amount of heats, produced from radiogenic heat, chemical reaction heat and nuclear fission heat, become the power sources for the geo-dynamo of great convection cell, which are the flows of the magma and the solid rock migrating up to the crust and down across the CMB to the F-layer. Based on the new conception calculates the data of the Earth, and compares with the existing current data. The insufficient mass and moment of inertia are the missing matters, which are taken as the parts of dark matter. Apply a simplified method to evaluate the Earth's mass and moment of inertia that are found to be only 85.73% and 94.82% of the current data. By the insufficiencies of the Earth's data, a planet of dark matter has been calculated out, which is reasonably inside the Earth but other space than ours. The new conception may be confirmed from Chandler wobble, and some scientific problems can be roughly solved.

**Keywords** Dark matter, Multiverse, Density jump, Convection cell, Chandler wobble

---

### Introduction

In 1937, Caltech astronomer Zwicky, noticed that masses of nebulae were estimated either from the luminosities of nebulae or from their internal rotations, both methods of determining nebulae masses are unreliable. He surmised that the Coma cluster of nebulae was moving around so fast that some extra, hidden mass must be present to supply the gravitational glue [1].

In the 1970s, astronomers detected that when star outside edges of the Milky Way and other spiral galaxies were found to be orbiting faster than theory predict; individual galaxies, it seemed, also harbored a reservoir of unseen matter whose gravity kept their stars from escaping[2]. The total mass of stars in a galaxy, which can be estimated by observing the galaxy with an astronomical telescope, is less than 10% of this total mass of the galaxy estimated from the orbiting stars. The phenomenon appears throughout the Universe. Unobservable matter, amounted to more than 90 % mass of the entire Universe, is called dark matter [3]. The dark matter is real that can only be detected by its gravitational influence on visible matter. While almost all astronomers agree on the existence of the dark matter; however, after more than 8 decades of search, there is nothing gained. Therefore, the dark matter is a major problem, which still has no solution.

In 1998, the High-Z Supernova Search Team published observations of type 1asupernova as standard candles [4], and in 1999 the Supernova Cosmology Project followed immediately [5], then the two independent projects obtained results suggesting a totally unexpected acceleration in the expansion of the Universe. In order to



explain the phenomenon of the Universe is expanding at an accelerating rate, "dark energy" is the most accepted hypothesis to the observations. Dark energy acts as a sort of an anti-gravity and is responsible for the present-day acceleration of the Universal expansion.

In 2012, the Wilkinson Microwave Anisotropy Probe (WMAP) has refined its measurements with a final data of the present-day Universe: 4.63% normal (baryonic) matter, 23.3% dark matter and 72.1% dark energy [6]. In 2014, the Planck Cosmology Probe released the new estimated content of dark matter 26.8 %, dark energy 68.3 % and normal matter 4.9 % in the Universe [7]. Roughly there are dark energy 68%, dark matter about 27%, and the rests — everything ever observed with all of our instruments and all normal matter — add up to less than 5% in the Universe.

In 2010, astronomers, Sawangwit and Shanks, in the Physics Department at Durham University, used astronomical objects that appear as unresolved points in radio telescopes to test the way the WMAP telescope smoothed out its maps. They find that the smoothing is much larger than previously believed, suggesting that its measurement of the size of the CMBR (Cosmic Microwave Background Radiation) ripples is not as accurate as was previously thought, which in turn makes the standard model of the Universe open to question [8]. If true this could mean that the ripples are significantly smaller, which could imply that dark matter and dark energy are not present after all.

Dark energy is a current scientific hypothesis, being neither matter nor radiation, its physical properties have no any clue, and we don't know how it works, and dark matter is also no solution, so, now all astrophysicists take them as the major problems.

### **Ten-dimensional space-time of String theory reveals multiverse**

In order to address these questions of astrophysics, in 1970s String theory was introduced. There are two theoretical framework in String theory: one is called Superstring theory [9] that requires 10 space-time dimensions, and the other is called M-theory [10, 11] that originates from a more fundamental 11-dimensional theory.

The origin of String theory is based on the Universe constitution of nine-dimensional space and one-dimensional time. String theory has been strictly proved a mathematical theory that is currently the only one can unify the four fundamental forces of nature, and potentially provides a unified description of gravity and particle physics. The starting point for String theory is the idea that the point-like particles of particle physics can also be modeled as one-dimensional objects called strings. The characteristic length scale of strings is assumed to be on the order of the Planck length, or  $10^{-35}$  meters that looks just like an ordinary particle, with its mass, charge, and other properties determined by the vibrational states of it in different ways. One notable feature of String theories is that these theories require extra dimensions of space-time for their mathematical consistency. The 10-dimensional space-time of the String theory is interpreted as the product of ordinary 4-dimensional space-time and a 6-extra-dimensional spaces, which is as yet unobserved [12].

String theory is now not established as well as Relativity theory, because there is no the exact boundary condition to fit the real Universe and works out a theoretically solid basic geometry, though many mathematicians and physicists have attempted to compactify the constitution of ten-dimensional space-time model through spontaneous symmetry breaking, to a four-dimensional one as our known world and 6-extra-dimensional space, which is compacted to be tiny space called Calabi-Yau space as Plank space ( $10^{-35}$  m), but no proposed method meets perfection.

In the multidimensional theories of String theory, the force of gravity is the only force of nature with effect across all dimensions. This explains the relative weakness of gravity compared to the other forces of nature (as electromagnetic wave) that cannot cross into extra dimensions. In that case, dark matter could exist in extra dimensions that only interact with the matter in our space through gravity. That dark matter could potentially aggregate in the same way as ordinary matter, forming extra-dimensional galaxies [13]. To date, no experimental or observational evidence is available to confirm the existence of these extra dimensions.

In 2004, Dvali suggested that the extra dimensions of space does not curl up (not compactified) becomes minimum, but infinite in size and uncurved, just like our ordinary three-dimensional view [14]. Character in String theory, they rethink the "extra dimension" problem, that is, gravity can roam to an additional dimensions of space. They think that the accelerated expansion of the Universe is not caused by dark energy, but because



gravity leaks out of our world. In particular, the theory predicts that the Universe has extra dimensions into which gravity, unlike ordinary matter, may be able to escape. This leakage would warp the space-time continuum and cause cosmic expansion to accelerate. Thus the extra dimensions need not be small and compactify, but may be large extra dimensions; i.e., outside our ordinary three-dimensional space, there are the same six extra dimensions of space in the Universe.

Without breaking the nine-dimensional space of the Universe down, the ten-dimensional space-time is considered to universally exist. According to “Causality Principle”, an effect cannot occur before its cause, which means time has a direction and cannot be divided into some different parts. So one-dimensional time is taken as a common standard in order of event in the Universe. According to “Anthropic Principle”, which is the simple fact that we live in a Universe set up to allow our existence. It means that three-dimensional space and one-dimensional time are taken as one Universe as our living world. Therefore, the nine-dimensional space can be divided into three portions, and each portion has a common standard time. It mean there are three-cosmic framework in the Universe, called triple Universes or multiverse, which cannot be observed directly with one another.

In 2002, the Planck space map of cosmic background radiation shows a stronger concentration in the south half of the sky and a ‘cold spot’ that cannot be explained by current understanding of physics. In 2005, Laura Mersini-Houghton, theoretical physicist at the University of North Carolina, and Richard Holman, professor of Carnegie Mellon University, predicted that anomalies in radiation existed that can only have been caused by the gravitational pulling on our Universe from other Universes as it formed during the Big Bang [15]. It is the first ‘hard evidence’ that other universes exist has been found by scientists, and it accords with the three-cosmic framework of the Universes.

In 1957, Princeton University Dr. Everett devised “the many-worlds interpretation (MWI) of quantum mechanics” [16]. The core of the idea was to interpret in the quantum world, an elementary particle, or a collection of such particles, can exist in a superposition of two or more possible states of being. An electron, for example, can be in a superposition of different locations, velocities and orientations of its spin. Yet anytime scientists measure one of these properties with precision, they see a definite result—just one of the elements of the superposition, not a combination of them. Nor do we ever see macroscopic objects in superposition. The many-worlds interpretation is a theory of multiple Universes [17].

Most cosmologists today accept this type of multiple Universes. According to String theory, the three-cosmic framework of the Universes have characteristics in which each Universes describes a world of general matter and the others describe another world, which we know nothing. Among any another worlds, there is no basic interactive forces of nature except gravity; in other words, the theoretic graviton in the field of gravity can penetrate all three Universes; however, the light (electromagnetic wave) cannot that means the dark matter may be situated in a Universes other than ours. The best method of exploring dark matter is to start from the Earth where we live.

### **Based on the multiverse exploring dark matter from the Earth**

In the current Earth model utilized in seismological investigations, such as body-wave travel times, surface-wave dispersion and free oscillation periods for researching the chemical composition and the density distribution of the Earth, the portions of the crust and the upper mantle have been analyzed with satisfactory accuracy. Regarding the lower mantle and the core portion, however, there remain a number of questions to be answered. It has been well known that there are two convections circulating individually below the crust to the lower mantle and in the outer core itself. The mantle and the core are not in chemical equilibrium and the fine structure of the core-mantle boundary (CMB) is not well understood. Although some hypothesizes such as the existence of a D'' layer in the lower mantle and iron combined with oxygen as the primary alloying constituent of the outer core are suggested, and a lot of advances of this research have come out, but there are also some discrepancies in the interior of the Earth [18, 19]. Furthermore, there is no conclusive evidence that the inner core is in thermodynamic equilibrium with the outer core. The main problem is a lack of phase equilibrium data for plausible core compositions at the appropriate conditions, added to the fact that seismological observations do not yet offer a decisive constraint on the difference in composition between the inner and outer core [20]. In order to investigate the outer core, a different view of the deep interior of the Earth should be taken to analyze



the Earth's constitution, composition, temperature and pressure, and a revolution in the chemical composition should be developed.

### The arguments at the core mantle boundary

With regard to the Earth's interior, the constitution of the deep interior is uncertain with some difficulties. In order to conduct further investigation, the Preliminary Reference Earth Model (PREM) [21] is taken as the current Earth model in this paper. At the CMB of this model, the solid portion of the lowermost mantle has a density of  $5.57 \text{ g/cm}^3$ , which jumps to  $9.90 \text{ g/cm}^3$  in the liquid portion of the top core, a density jump of 77.74 %. However, in the PREM the density jumps significantly at the CMB, all investigations cannot confirm the data directly, so, research about the interior constitution of the Earth is needed, especially at the CMB.

Deducting the certain quantities of the crust and the mantle portion from the known data of the mass and the moment of inertia of the Earth, there are the great amounts of rest values. In order to match it, the ordinary way is to set a distribution of high density in the core and also a high density jump at the CMB. There as on is considered as a matter of course within the domain of current science. If the factor is not initially taken into consideration, a different conclusion may be drawn. There are some arguments in the topic of the CMB as follows:

1. Ramsey [22] and Lyttleton [23] have challenged the concept of an iron core. They suggest that the silicates (iron silicates and magnesium silicates) are the main composition of the mantle. Because the solid mantle under high temperature and high pressure at the CMB, the mantle silicates undergo phase-changes, which are called Ramsey' s phase-changes, a solid phase changing into a liquid phase in the top core, to produce the material of high density, low melting point and electrical conductivity. Ramsey's hypothesis is still accepted by a few geophysicists for several reasons.

2. Knopoff [24] showed that cross a phase transition near the surface of CMB, one can predict that the bulk modulus  $K$  increases by the increasing of the density  $\rho$ ; in such a way, the ratio  $K/(\rho^{7/3})$  is kept constant. From the models, the bulk modulus remains essentially unchanged across the CMB that is difficult to account for a large density jump from about  $5.57 \text{ g/cm}^3$  to about  $9.90 \text{ g/cm}^3$  in the PREM. On this basis, it is difficult to argue in favor of the density distribution to be smoothly continuous at the CMB and the composition of outer core is silicates.

3. Bookbinder [25] studied the variation in amplitude, with an epicentral distance  $\Delta$ , of the reflected phase  $PcP$ . Calculations of reflection coefficients at a plane solid-liquid boundary show that a model with  $P$  and  $S$  velocities at the bottom of the mantle of  $13.64 \text{ km/sec}$  and  $7.30 \text{ km/sec}$ , respectively; with a  $P$  velocity at the top of the core of  $7.5 \text{ km/sec}$ ; and with a ratio of core density to mantle density of  $1.0$  will satisfy the observations of amplitude and change of initial phase of  $PcP$ . A range of similar models with velocities at the top of the core down to  $7.2 \text{ km/sec}$  and density ratios as high as  $1.05$  will also satisfy the observations. He found that the amplitude-distance curve, which displays a minimum at  $\Delta = 32^\circ$ , was not consistent with the computed reflection amplitudes for a solid-liquid interface, if the previously accepted values of  $P$  velocity and density were employed. A model is proposed that is consistent with the observed amplitudes, provides no discontinuity in density between the low mantle and the core. Amplitude observations of  $PKKP$  phases also satisfy the model. Such a model may arise if there is considerable mixing of the core material with the lowermost mantle, and vice versa.

From the items of 1, 2 and 3 above, the descriptions can be initially identified that the materials of mantle and core mixing with each other, and the density distribution between the lower mantle and the outer core should be continuity in order to solve some problems in the geophysics. The main composition of the outer core should be considered as the same ingredients of molten rock and/or mineral silicates, which are chemically consistent with the same ingredients of the lowermost mantle, and may be not liquid iron.

Iron is the richest nature metal element in the Universe. Because of the Earth's interior mass, density distribution and average density, it is needed an iron element to explain the composition of the core. However, this does not mean that we have proved that the core is made of "iron" parts. The materials of mantle and core based on "Birch Diagram" [26], which was inspected the relations of "velocity/density" in each element, to indicate the composition of matter. These claims are the Earth Sciences today on the "golden rule". By "Birch Diagram" speculated that the core is mainly composed of "iron", but that's just an assumption, we cannot examine it [27].



The composition of the Earth by the proportion of the meteorites that fall to the ground, can be found the more stone meteorites on Earth, iron meteorite contains only about 15%. The planet Earth basically gathered from small particles of the same cold solid ingredients, therefore did not at any stage possibly in the interior of the Earth to develop into an iron core. If by the primary reference earth model (PREM) calculate the mass of iron core part of the Earth that is about one-third of the Earth's. It is share of iron meteorite much large than the iron meteorite containing 15%, apparently not reasonable. So, does the core, particularly the part of liquid outer core, fills with iron? It is worth exploring. So, the outer core need not be filled with iron, perhaps as the mantle may be mineral silicates.

### Topography of CMB reveals both sides at CMB to be the same materials

A sufficient quantity of high-quality digital data from two global networks: a network for very long period seismology [28] and the seismic research observatory [29] began operation in the mid-1970s and developed about three decades provided the framework of formal analysis, and the availability of computers, made feasible the handling of immense amounts of data and the large-scale calculations necessary in three-dimensional problems. Geophysicists recorded on Earth more than 15,000 times magnitude 4.5th-class earthquake data, input seismic laboratory computer, drawing the three dimensional topographical map of the Earth's Interior, and computer tomography X-ray photograph, produced the CMB topography, which is found in boundary of solid mantle and liquid outer core. The undulations of CMB in regions from 3,000 km to 6,000 km, denote the irregular high mountains and deep valleys. The amplitude of the boundary is  $\pm 6$  km, in other word, the height difference more than 10 kilometers, even higher than the world's highest peak—Mount Everest, and in a very unstable state [19].

In three-dimensional maps, tomographic models represent an instantaneous, low-resolution image of a convection system. Detailed interpretation knowledge of mineral and rock properties as yet poorly known that are required. Maps of CMB topography have been derived on the basis of seismological inversions of long wave travel-times to construct three-dimensional maps with the magnitude of amplitudes from  $\pm 3$  km up to  $\pm 6$  km (relief 12 km) and with 3000~6000 km scale lengths [18-19, 30-41]. The CMB topography is different from that predicted by the hydrostatic equilibrium theory and exceeds the inferences from geodesic studies. If we doesn't address the effects on CMB topography to get the smaller peak, the amplitudes of CMB topography should be large than  $\pm 5$ km, so, the relief of 10 km is taken as an average value to discussion.

A complex set of constraints on the possible modes of convection in the earth's interior has not yet been worked out; this will require numerical modeling of convection in three dimensions. Thus the interpretation of the geographical information from seismology in terms of geodynamical processes is a matter of considerable complexity [42]. The topography on the CMB can be sustained only by dynamic processes, and these processes must be crucially understood. Despite the general agreement on the overall shape of CMB undulations, these details of the peak-to-peak amplitude and pattern are still debated [41]. Geoscientists used PcP, PKPbc, and PKKPbc phases selected from the data set by Engdahl *et al.* [43] and concluded that CMB topography cannot be resolved [38]. At present, consensus regarding the regional pattern of the CMB topography, as well as on its peak-to-peak amplitude is lacking [44].

In 1987, Bloxham and Gubbins argued that flow near the core surface may be controlled by lateral temperature variations in the lowermost mantle, which are amply sufficient for this to be a significant effect [45]. But Stevenson inferred the lateral temperature variations near the outer core surface are very small, amounting to only a few millikelvin, based on  $\alpha = 5 \times 10^{-6} \text{K}^{-1}$  ( $\alpha$  is coefficient of thermal expansion) [46]. The lateral temperature variations are so small that it should not affect the flow near the core surface, and the pattern of topography of the core-mantle boundary are determined by processes in the core [19].

An approximate analysis is given for the likely fractional lateral density variations ( $\delta\rho/\rho$ ) in the outer core, caused by large scale-length fluid dynamical processes. It is first shown that fractional density and fractional seismic velocity variations are probably comparable, so that fluid dynamic arguments have relevance to seismic data. In regions of nearly neutral stability in the outer core, an analysis of convective vigor indicates an upper bound of  $|\delta\rho/\rho| \leq 10^{-8}$ . Scientists undertaking analysis of the Earth's seismic travel times or normal modes can safely assume that there are negligible lateral variations in the outer core [46].





According to the PREM, iron is the major component of the core, and there is a density jump of 77.74 % at the CMB. Neglecting the gravity anomaly, the pressure of lateral difference at the lowermost level of the CMB is 4.246 kbar considering a relief height of only 10 km. This pressure can produce an increasing iron density of  $6.323 \times 10^{-3} \text{ g/cm}^3$  under conditions at the top of core, and yields a fractional lateral density variations of  $\delta\rho/\rho = 0.639 \times 10^{-3}$ , which is far beyond the upper bound of fractional lateral density variations  $10^{-8}$  [19].

In three-dimensional maps of the Earth's interior, the topography of the CMB is different from that predicted by the hydrostatic equilibrium theory, which contains information important to geodynamic processes and the geomagnetic secular variation. The topography on the CMB is likely to result from convection in the overlying mantle [47]. Ruff and Anderson (1980) argue for dynamo action in the core maintained by differential heating of the core by the mantle [48], and some agreements of that are probably determined by processes in the core [49]. The depressed regions of the topography are dynamically supported by down welling of cool mantle material [50]. Obviously the relief is dynamically supported and provides coupling between the solid mantle and the fluid core.

The scientists undertaking analysis of the Earth's geoid or seismic travel times or normal modes can safely assume that there are negligible lateral density variations in the outer core. The lateral density differences in the top of outer core are so small that it could not provide a relief in excess of 10 km at the CMB, which is related to mantle temperature, and suggest further effects due to topography associated with subduction slabs, and may have a mechanical rather than thermal effect on the flow [51].

It is obviously in terms of the geodynamic processes that only the vertical interactions of material and the temperature between the lowermost mantle and the outer core are the main cause. In order to maintain the 10 km of relief, the density difference between the liquid state and the solid state at the CMB must be very small. There is a significant suggestion that the density of the materials between the both sides at the CMB must be similar or equal; i.e., the hypothesis that the same materials between a solid mantle and a liquid core change states with each other at the CMB to produce topography of the CMB more than 10 km relief.

Therefore, the density jump of 77.74 % at the CMB of the PREM may be considered as an unreasonable basis of reference. Thus based on the topography, the idea of a spherical structure of the CMB in the Earth model has been challenged. Therefore, a new study is necessary to determine the actual Earth's model.

### **The great convection cell spanning the crust through F-layer**

In 1971, geophysicist Morgan proposed the hypothesis of mantle plumes, which generated from thermal boundary layers have been invoked for decades to explain the formation of hotspots and flood basalts provinces on the Earth [52]. In this hypothesis, convection in the mantle transports heat from the core to the Earth's surface in thermal diapirs. There are two largely independent convective processes occur in the mantle. 1. *Mantle plumes*, which carry heat upward in narrow, rising columns, driven by heat exchange across the core-mantle boundary to the crust. 2. The broad convective flow associated with *plate tectonics*, which is driven primarily by the sinking of cold plates of lithosphere back into the mantle [53].

The interior heat gives rise to convection currents in the Earth's mantle, energized by the heat emitted by the core. Various lines of evidence have been cited in support of mantle plumes. Plate tectonics is a scientific theory describing the large-scale motion of Earth's lithosphere. Tectonic plates builds on the concept of continental drift, and has to be accepted by the geoscientific community after seafloor spreading was validated.

Mantle plumes are tubes of hot rock rising from Earth's core, many of them underneath known volcanic hot spots at Earth's surface. The plumes are fatter than expected, which means that they carry more heat away from Earth's core, an indication that plumes are important for cooling the planet of Earth [54].

Earth's internal heat powers most geological processes and drives thermal plumes through convection or large scale upwelling and doming. However, no plume has yet been found to satisfy all the criteria currently attributed to plumes, adding that the hypothesis has become too flexible, with ad hoc variations tacked on to accommodate any finding [55]. It is still unresolved whether features that have been attributed to plumes are primarily the result of plate tectonics and stress, or fluid dynamics and high temperature, and the factors of plate movement is unclear, and still the subject of much debate. With uncertainty in the areas of lower mantle and outer core, and possible unrecognized complexity, precision in the estimates of CMB heat flux is not yet clearly in hand.



The heat loss from the Earth's surface is more than the heat getting from the Sun. If the core does not for the continued release of heat, the Earth would have cooled off and become a dead rocky globe like as Mars or Moon. Releasing heat as we know is by the nuclear energy from the much slower decays of radioactive elements like as  $^{238}\text{U}$ ,  $^{235}\text{U}$ ,  $^{232}\text{Th}$ , and  $^{40}\text{K}$  [56], gradually, however, radiogenic heating generated in the core turns the iron into a convecting geo-dynamo that maintains a magnetic field strong enough to shield the planet from the solar wind. This heat leaks out of the core into the mantle, causing convection in the rock that moves crustal plates and fuels volcanoes.

In 1997, it became possible that using seismic tomography to image submerging tectonic slabs penetrating from the surface all the way to the core-mantle boundary [57]. Hotspots power the volcanic activity that is continuing to produce basalt-lava, which forms the Hawaiian Islands and Iceland. Norwegian scientists discovered that basalt eruptions in the Hawaiian Islands and in Iceland varied significantly over time [58]. Seismic tomography appears to image vertical, column-like heat paths extending to the edge of the core for each of those hotspots. As the two hotspots are located on opposite sides of the globe, Mjælde, Wessel and Müller suggest the co-pulsations are a global hotspot phenomenon that appears to represent changes in heat from the Earth's core [59].

The current total heat flow at Earth's surface estimates to be refined and are agreeing at around 43-49 TW (terawatts) [60- 64], involves contributions from secular cooling, radiogenic heating from decay of  $^{238}\text{U}$  and  $^{232}\text{Th}$ , heat entering the mantle from the core, and various minor processes such as tidal deformation, chemical segregation and thermal contraction. Most models assume a CI carbonaceous chondrite origin for the Earth, leading to a total heat production in the silicate Earth (mantle plus crust) of about 20 TW [65], estimates of mantle primordial heat loss range between 7 and 15 TW [66]. The heat flow across the CMB cannot be greater than 29 TW, a value obtained in the case of a steady mantle temperature.

The radioactive power of the planet is predicted a range of radioactive powers, overlapping slightly with the other at about 24 TW, and together spanning 14-46 TW. Approximately 20% of this radioactive power (3-8 TW) escapes to space in the form of geo-neutrinos. The remaining 11-38 TW heats the planet with significant geodynamical consequences, appearing as the radiogenic component of the 43-49 TW surface heat flow. The non-radiogenic component of the surface heat flow (5-38 TW) is presumably primordial, a legacy of the formation and early evolution of the planet [66].

Intimately related to terrestrial radiogenic heating is a flux of electron antineutrinos, commonly called geo-neutrinos [67]. Beta decays of daughter nuclides in the radioactive series of  $^{238}\text{U}$  and  $^{232}\text{Th}$  produce detectable geo-neutrinos. Geo-neutrino observatories lead to estimate the radiogenic heat production. Geo-neutrino observatories operate underground at two Northern Hemisphere locations in Japan [68] and Italy [69,70], monitor large volumes of organic scintillating liquids for the delayed coincidence signal, indicative of electron antineutrino quasi-elastic scattering on protons. Existing observations with limited sensitivity to geo-neutrinos from the interior of Earth constrain radiogenic heating to 15-41 TW [66], assuming a thorium-to-uranium abundance ratio ( $\text{Th}/\text{U} = 3.9$ ) and a homogeneous mantle. The radiogenic heating of 15-41 TW is very close to the predicted range of 14-46 TW.

Nuclear energy generated in the core from the radioactive elements not only slower decay but also faster fission. Kuroda [71] applied Fermi's nuclear reactor theory [72] and demonstrated the feasibility that seams of uranium ore could engage in neutron-induced nuclear fission chain. In 1972, French scientists Francis Perrin discovered the intact remains of a natural nuclear fission reactor in a uranium mine at Oklo, in the Republic of Gabon, that had operated just as Kuroda had predicted. Oklo is the only known location for this in the world and consists of 16 sites at which self-sustaining nuclear fission reactions took place approximately 1.7 billion years ago [73,74]. Oak Ridge National Laboratory used computer programs to calculate the operation of different types of nuclear fission reactors that showed the geo-reactor would function as a fast neutron breeder reactor over the entire existing time of the Earth [75].

Geomagnetic field reversals and changes in intensity are understandable from an energy standpoint as natural consequences of intermittent and/or variable nuclear fission chain reactions deep within the Earth. Moreover, deep-Earth production of helium, having  $^3\text{He}/^4\text{He}$  ratios within the range observed from deep mantle sources, is demonstrated to be a consequence of nuclear fission. Numerical simulations of a planetary-scale geo-reactor were made by using the SCALE sequence of codes. The results clearly demonstrate that such a geo-reactor near



or at the center of the Earth would function as a fast-neutron fuel breeder reactor; and would function in such a manner as to yield variable and/or intermittent output power [75].

Geo-reactor-heat produced by nuclear fission can be variable, unlike heat from the natural decay of long-lived radioactive isotopes, which is essentially constant, decreasing slightly over very-long periods of time. Antineutrino measurements to date have not refuted the existence of the geo-reactor, but set an upper limit of 3 TW on its energy production [68] that does not include the contribution from radioactive decay energy of the geo-reactor's associated uranium.

As previous statements, the core is the most abundant in heat flow that part of it is thought to represent power dissipated by the geo-dynamo, and to produce the geomagnetic field [76]. A nuclear fission geo-reactor is clearly an acceptable alternative energy sources, and its output can be variable and/or intermittent, a fact that is quite consistent with the observed variability of the geomagnetic field [75]. Heat flow from the core is necessary for maintaining the convecting outer core and the geo-dynamo and Earth's magnetic field, therefore primordial heat from the core enabled Earth's atmosphere and thus helped retain Earth's liquid water [77].

At least some of the 2 million cubic kilometers of lava which spread over parts of Siberia 250 million years ago came from the lowermost mantle, up to 2900 kilometers below the Earth's surface. A small fraction of the rare and valuable metal platinum under 1 percent were discovered under the frozen wastes of Siberia may have come from the core [78]. Two studies support it: (1).from the US and Russia report, the ratio of helium-3 to helium-4 in Siberian rocks is up to 12.7 times the atmospheric value. Primordial helium-3 leaked away from the surface of the young Earth but was retained in the lower mantle. High helium-3 levels had been found earlier in hot-spot lavas, indicating the lava came from the lower mantle [79]. (2). unusually high levels of osmium-187 have been found in sulphide rocks in the deposits. The extra osmium probably came from the decay of radioactive rhenium-187, which is thought to exist in high concentrations in the metallic core [80]. Thereby some materials are found in the deposits come all the way from the core. On the basis of some of the metal platinum in Siberia may have come all the way from the core of the Earth, the idea of D''layer, which is considered to be virtually isolated the core from the rocky mantle and to sustain the chemical and the thermal equilibriums between the mantle and the core, may be challenged.

In 1991, Knittle and Jeanloz suggest that a significant amount of the energy driving mantle convection is generated in the core [81]. Checking the temperature of Earth interior, the hottest point is the center of Earth about 7000°C [82], and in the inner-core boundary over 6000°C [83],and in the CMB about  $4180 \pm 150$ °K [84], the abundant heat flow must from fluid core leaks out into mantle. In the higher resolution models, some of the heterogeneities extend upward from the CMB into the mantle in a manner suggestive of rising plume structure [47]. Thermal plumes are tubes of hot rock rising from Earth's core, and carry more heat away [54], On this basis, a great quantity of magma heated by the extreme temperatures in the core solidifies into rock and produces the heat of solidification at the CMB. A few quantity of magma absorbing this heat does not solidify, but mixes with masses of rock as honeycombed blobs of rock and brings some materials, including magma, osmium-187, <sup>3</sup>He and a little metal as platinum, rising upward at approximately an inch a year through the mantle to pour out at cracks in the mid-ocean ridge to form new ocean floor or in the continent to form great rifts, to disperse the internal heat on the Earth's surface that works as a secular cooling of the Earth. Approximately 80 % of the hot spots at the Earth's surface are manifestations of plumes rooted in the deepest part of the Earth. The outflow of heat is the dynamic source of continental drift.

Nevertheless, due to geological processes, the downward migrating masses of cold lithosphere plate in subduction zone of the crust may be driven through convection falling subduction slab all the way through the warmer surrounding mantle to the CMB. The downward masses of slab in the cold regions of the low mantle produce depressions of the CMB into the core, and both the cold region in the mantle and a depression of the CMB produce down welling flow in the core [49].

The depressed regions of the topography on the CMB are dynamically supported by down welling of cool mantle materials [30,50], and then through CMB into liquid core that are probably determined by processes in the core [49]. In the outer core materials absorb the abundant heat flow, and forms an upward convection thermal plume again. Obviously the relief of CMB is dynamically supported and provides coupling materials between solid mantle and fluid core.





In this way, the materials of lower mantle and outer core mixing with each other, and the density distribution between both should be continuity in order to solve some problems in the geophysics. The main composition of outer core should be considered as the same ingredients of molten rock and/or mineral silicates, which are chemically consistent with the same ingredients of lowermost mantle.

The energy source and buoyancy source in the core are still not well understood, but we attempt to explain this phenomenon from the perspective of convection cell. The downward masses of slab absorb the heat of fusion, diminishing the heat energy at the CMB, and melting in the core where viscosity is so high that the large quantity of molten rock may not diffuse but still remain a whole. So, the components of molten rock are seldom involved in the chemical reactions.

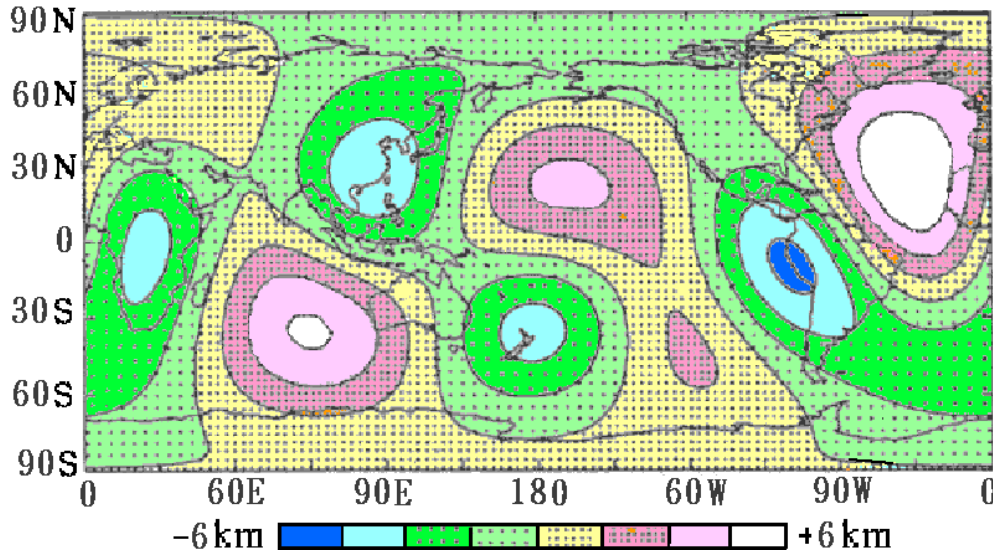


Figure 1: Topography CMB obtained by inversion of the combined PcP and PKP<sub>BC</sub> Data set [19]

According to mechanics, although the velocity of downward migrating flow is low, the mass of the slab column from the crust to the CMB is so large that its downward momentum has a great quantity. In the liquid outer core, there is no rigid body having enough mass to counteract the downward momentum, so the molten rock sinks all the way into the lowermost fluid core. The great downward momentum is counteracted merely by the solid inner core, which Jeanloz and Wenk have obtained a possible evidence of low-degree convection like it in the mantle in the inner core from an enigmatic observation [85].

Seismological studies indicate that the inner core of Earth is anisotropic for *P* waves, and has low *S* wave velocity, and high seismic attenuation. The presence of a volume fraction of 3 to 10% liquid in the form of oblate spheroidal inclusions aligned in the equatorial plane between iron crystals is sufficient to explain the seismic phenomena. The liquid could arise from the presence a "mushy zone" of dendrites or a mixture of elements other than iron that exist in liquid form under inner-core conditions [86]. Bergman [87] and Shimizu *et al.* [88] suggest that a thin mushy layer develops underneath the inner core boundary while the materials of outer core solidify onto the inner core. So, the inner core should be not a rigid spheroid.

The inner core rotation and high-quality teleseismic waveform doublets make the precise mapping of the topography of the inner-core boundary up to about 3.7 to 5.2 km. Dynamic models include a bumpy ICB rotating with the inner core itself or a transient slurry boundary containing a mixture of molten materials and solidified patches of iron crystals, which is rapidly modified by the turbulence at the base of the convecting outer core [89].

At the ICB, the momentum from the downward molten rock is transmitted through the inner core, the Earth's center, and probably on to the opposite side of the CMB. This phenomenon can be inspected by the three-dimension topographic map of CMB in the Earth (Figure 1) [19]. All these it is magma that sinks toward ICB, and its kinetic energy becomes the pressure and spreads into the earth's inner core, and pushes and shoves the relative opposite side of the ICB, even to form the unsmooth CMB. From the diagram, the CMB is concaving in New Zealand, but protruding in the North Atlantic Ocean, and concaving under the west coast of South



America, else protruding in region of Western Australia and near the Indian Ocean, and concaving under South Africa, also protruding in North Pacific Ocean too.

There is a significant suggestion that the same materials, dominantly silicates, of the rocky mantle and the liquid outer core change states with each other at the CMB to produce the relief of CMB topography over 10 km. A reasonable way may be figured out that the migrating rock or molten rock of plate sinks downward and magma or thermal plume rises upward in the great convection cell spanning the crust through the F-layer of outer core. A schematic diagram of the scenario is shown in Figure 2.

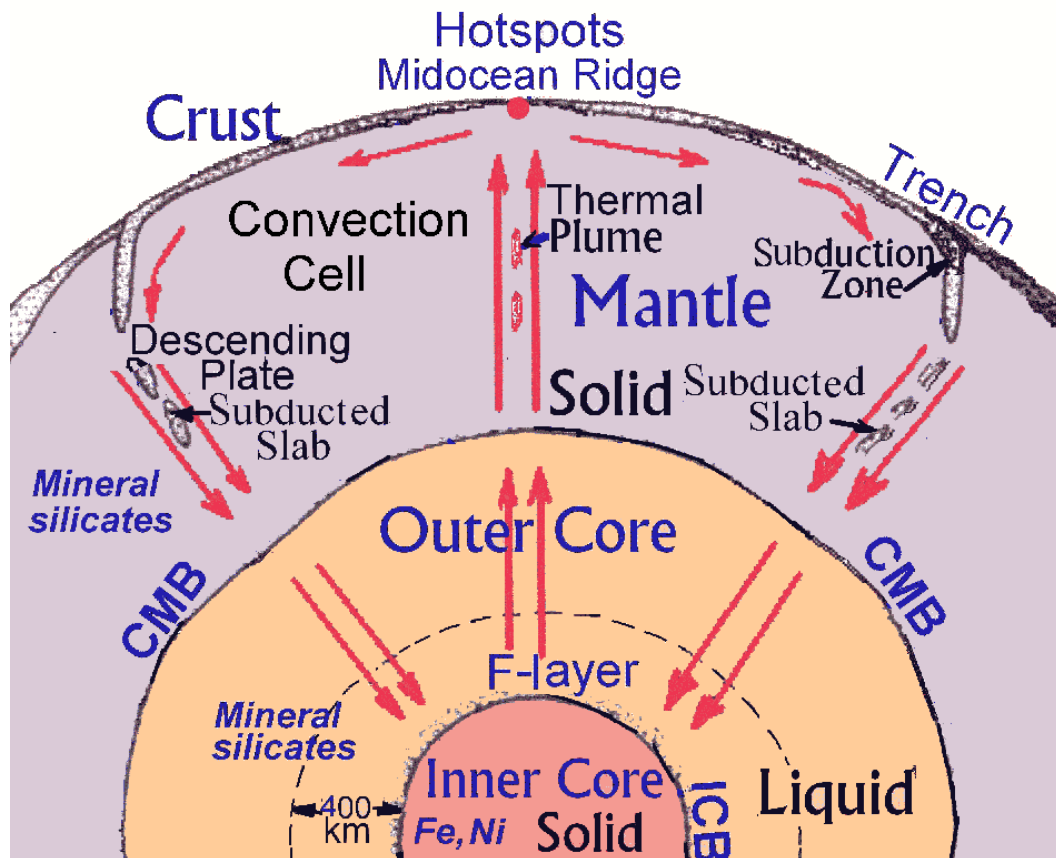


Figure 2: A schematic diagram of the great convection cell: the thermal plume migrates up to the crust and subducted plate down to the F-layer of outer core and causes a relief of CMB topography over 10 km

### The arguments at the inner core boundary

The seismic structure of Earth's inner core is highly complex, displaying strong anisotropy and further regional variations. However, few seismic waves are sensitive to the inner core and fundamental questions regarding the origin of the observed seismic features remain unanswered [90]. It is well accepted that the inner core solidifies from the outer core, but the details of this process are still largely unclear [91].

Seismologists have yet to answer some of the most fundamental questions concerning the core, one is the nature of the low-velocity gradient region at the lowermost outer core. A large number of seismological studies have suggested that the region just above the inner core boundary (ICB) is distinct from the rest of the outer core. The layer about 400 km above the ICB was originally termed the F-layer and was characterized by a strong low velocity zone [92]. After the research of velocity and amplitude in the core, scientists infer the high separated solutions of the F-layer is around the ICB [93-94]. Most observations indicate that the F-layer is global and surrounds the entire inner core [95-98].

From ray theory, an evidence of reduced seismic wave velocity gradient to near zero in F-layer of outer core has been interpreted [99-100]. Later Earth models, constructed with more accurate travel time data, instead defined this as a region of increased velocity. Among velocity models at the base of the outer core reported by different studies (e.g.: Qamar [94], Dziewonski & Anderson [19], Choy & Cormier [101], Souriau & Poupinet [96], Song



& Helmberger [102], Kennett *et al.* [103] and Yu *et al.* [104]), the main difference is the structure of the velocity and its gradient at the bottom 400 km of the outer core. According to the Earth's models, such as: AK135 [103], PREM2 [102], and Jeffreys-Bullen model [92], Bullen & Bolt [105] denote a low-velocity gradient region at the lowermost outer core. In PREM [21], the velocity increases with a nearly constant gradient around  $0.6 \times 10^{-3} \text{ s}^{-1}$ . In PREM2 and AK135, the velocity gradient decreases from about  $0.6 \times 10^{-3} \text{ s}^{-1}$  at 400 km above the ICB to nearly zero at the ICB, and the velocity profile with depth is more flat than that in PREM (Figure 3). Therefore, 400 km above the ICB is chosen as the minimum 'pinning depth', at which the models are evaluated and constrained to agree with PREM in value and gradient.

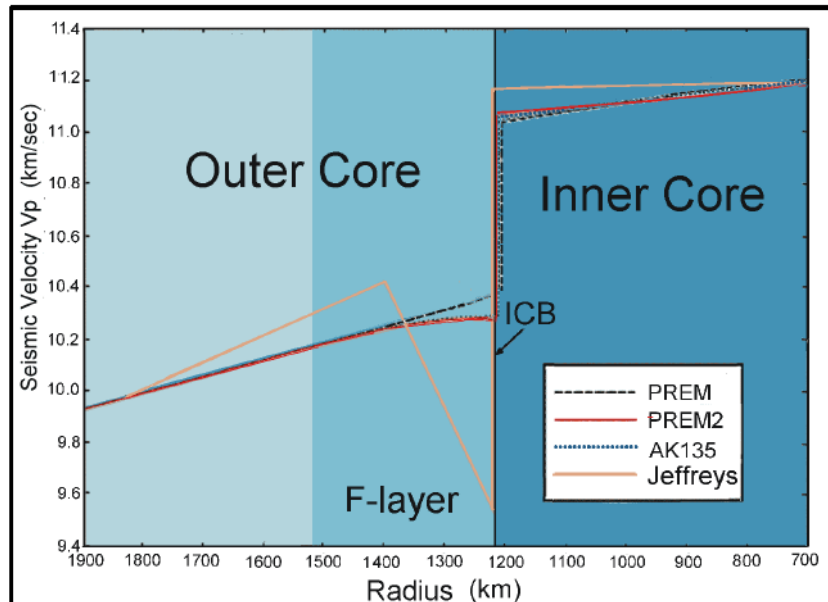


Figure 3: A comparison of seismic  $P$  velocity ( $V_p$ ) and  $S$  velocity ( $V_s$ ) distributions is given among the Earth models of Jeffreys-Bullen, Ak135, PREM2 and PREM. The comparison indicates that the velocity curves closely agree generally, but the main exceptions are that the low-velocity zone F-layer in the  $V_p$  curve

While the seismic wave enters F-layer, a sharp velocity discontinuity at ICB, the velocity jumped 0.78 km/sec, and a low velocity gradient at the base of the fluid core that indicates slightly different properties of the components. The most robust pointer to a viscosity at the bottom of the outer core may be still its reduced  $P$  velocity gradient, which is difficult to explain without appealing to the existence of a chemical boundary layer [102, 103]. These models imply that near the base of the outer core density increases too quickly to be explained solely by compression, and some sort of change in chemistry and phase may occur.

Experiments [106, 107] and numerical simulations [108] have shown that temperature anomalies generated by strongly heterogeneous CMB heat flux can be transmitted from the CMB to the ICB by outer core convection. As the Earth cooled and dissipated its internal heat toward the surface of the Earth through mantle convection, the geographical coincidence of the ICB and CMB anomalies may suggest strong thermal coupling of the mantle and the core that means there is a convection cell across CMB. The F-layer should have some functions instead that of the well-known  $D''$  layer, such as the thermal and chemical equilibrium.

The regional differences in  $PKiKP$ - $PKiKP$  travel times and  $PKiKP/PcP$  amplitude ratio data may originate from the F layer instead. Bolt and Qamar [109] first proposed the amplitude ratio ( $PKiKP/PcP$ ) technique and estimated a maximum density jump of  $1.8 \text{ g/cm}^3$  at the ICB. Bolt [93] clearly observed both low angle and steep incident reflections  $PKiKP$  of about one second period at the ICB. The mean amplitude ratio  $PKiKP/PcP$  suggests a density jump  $\Delta\rho$  of  $1.4 \text{ g/cm}^3$  here. Souriau and Souriau used the amplitude ratio  $PKiKP/PcP$  at short distances to constrain the density jump at the inner core boundary to be in the range of  $1.35 \sim 1.66 \text{ g/cm}^3$  based on array data [110]. Shearer & Masters used "non-observations" of  $PKiKP$  on the observed amplitude of this phase, leading to upper bounds  $\Delta\rho=1.8 \text{ g/cm}^3$  at inner core boundary on the corresponding  $PKiKP/PcP$  amplitude ratios [111]. Studies used  $PKiKP$  to calculate the density jump  $\Delta\rho$  across the inner core boundary, and



this has remained a topic of debate to the present day [112]. At the ICB, a density jump of  $0.68 \text{ g/cm}^3$  in the PREM is too small to compare with the previous data.

As stated previously, the difference in density between the outer core and the inner core must be great. Jeanloz and Ahrens [113] completed shock-wave experiments, in which it was found that the density of FeO is  $10.14 \text{ g/cm}^3$  when reduced to core temperature and 250 GPa pressure, and under the same conditions the density of Fe is  $12.62 \text{ g/cm}^3$  [114] when FeO becomes Fe. The difference between both is  $2.48 \text{ g/cm}^3$ , a figure higher than all of the other evaluated values.

From this information other than the PREM, the density jump between the lighter liquid outer core and the solid inner core seems to be too large to represent a simple volume change on condensing as the same major components change from a liquid state Fe into a solid state Fe. The composition of the outer core is not likely to be the same as the inner core, since a liquid in equilibrium with a solid phase in a multi-component system does not have the same composition as the solid [115]. We infer that the major component of outer core is mineral silicates, but iron in the solid inner core.

On the basis of the free oscillation periods, Derr has inferred an earth model DI-11 by least-squares inversion with an average shear velocity of  $2.18 \text{ km/sec}$  in the inner core and a jump in density of  $2.0 \text{ g/cm}^3$  at its boundary that satisfies the known mass and moment of inertia [116]. We use the largest density jump of Derr's suggestion  $2.0 \text{ g/cm}^3$  at the ICB to research the new earth model in this paper.

### Examining the chemical composition of the core

In order to confirm a favorable constitution of the Earth, the chemical composition of the core must be further investigated. The composition of the Earth's core is one of the most important and elusive problems in geophysics. There is no perfect explanation of the chemical equilibrium between the core and the mantle, and the inner core is not in thermodynamic equilibrium with the outer core [20].

The physical and chemical properties of the lower mantle are poorly known, and the understanding of the coupling mechanisms between the mantle and the core is poor on all timescales. But the CMB sets boundary conditions for processes occurring within the core that is a well-known fact. The topography and the lateral temperature variations in the lowermost mantle may have an indistinguishable effect on the magnetic field [45]. Secular variations with periods shorter than a million years, but longer than several years, almost certainly originate from processes operating in the outer core; unfortunately, there is not yet consensus as to what those processes are [117].

In three-dimensional maps, topographic models represent an instantaneous, low-resolution image of a convecting system. Detailed interpretation knowledge of mineral and rock properties that are, as yet, poorly known is required. A complex set of constraints on the possible modes of convection in the Earth's interior that have not yet been worked out; this will require numerical modeling of convection in three dimensions. Thus the interpretation of the geographical information from seismology in terms of geodynamical processes is a matter of considerable complexity. The topography on the CMB can be sustained only by dynamic processes, and these processes must be crucially understood [42].

The fine structure of the CMB is not well known, but it contains information important to the geodynamic processes in the mantle or in the magnetic field generated in the outer core [118]. Approaching the Problem of the CMB, Creager and Jordan studied travel-time anomalies of *PKiKP* and *PKP<sub>AB</sub>* and corrected for the mantle structure onto a region in the vicinity of the CMB [18]. They consider some hypotheses with regard to the source of anomalies that are the perturbations in the CMB topography. Based on the great convection cell a relief of the core in excess of 10 km provided by the three-dimensional maps may be accepted.

As stated previously, the main components of the outer core are similar to the main components of the lower mantle, i.e. mineral silicates. Based on mineralogy, the main mineral of the mantle is pyrolite, a compound of silicates, and the main components of the outer core are also pyrolite but only in a liquid state. Under the same conditions, the higher the temperature under which common minerals are produced, the lower the polymerization is and vice versa. The closer the crystal minerals of the mantle under the temperature and pressure are to the core, the more the polymerization losses of crystalline mineral. Then the bonding forces of mineral compound are destroyed and the crystallization gradually diminishes.



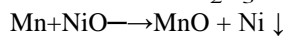
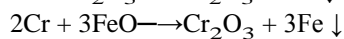
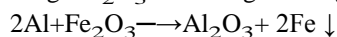
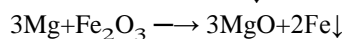
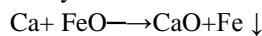
For example, olivine, an important rock of the Earth, under room temperature and pressure is a complex crystal tectosilicate. Quartz is a mineral of olivine. After heating, quartz, the four oxygen of the silicon oxygen tetrahedron and four different structures of the silicon oxygen tetrahedron, are gradually reduced to phyllosilicates, inosilicates and cyclosilicates, respectively. When the temperature raises considerably high, the four oxygen of silicon oxygen tetrahedron become an elemental unit of silicates known as sorosilicates. When the temperature approaches the melting point, the sorosilicates become the nesosilicates, which are the crystal tetrahedron of silica mineral, a basic structural unit of minerals.

At reaching the CMB, olivine reduces phyllosilicates, inosilicates, cyclosilicates, sorosilicates and nesosilicates respectively, when the temperature rises considerably high ( $4180 \pm 150^\circ\text{K}$ ) and reaches the melting point of solid rock, some of the rock melts in the core and liquefies into the molten rock [84]. In the F-layer of the deeper core, the high temperature more than  $6000^\circ\text{C}$  [83], polymerization may cease completely, and mostly bonding power of ions loses, only the electronic bonding force exists. All the ions and molecules may become unbounded. Therefore, the molten rock or magma becomes a mixture of oxides such as FeO, MgO, NiO, SiO<sub>2</sub>, Fe<sub>2</sub>O<sub>3</sub>, Al<sub>2</sub>O<sub>3</sub>, Cr<sub>2</sub>O<sub>3</sub>, etc., and metals, such as Fe, Ni, Mn, etc.

According to temperature profile of Earth's interior, the center of Earth is made up of high temperature material, which is the hottest point, estimated to be  $7000^\circ\text{C}$  [82] that is hotter than the surface of the Sun. In F-layer, the chemical components maybe reduce the viscosity, the full fluid oxides and metals are able to flow, and diffuse, float or sink more freely according to its specific gravity. Estimation of Fe melting temperature at ICB pressure based on static compression data spans the range  $6230 \pm 500^\circ\text{K}$  [119]. The F-layer above the ICB, in which Fe likes snow flake falling in the inner core [120].

There are a large amount of iron oxides (FeO, Fe<sub>2</sub>O<sub>3</sub>) in the mantle, and the deeper the mantle, the higher the proportion of iron oxides is. An iron oxide which has metal-like density and electrical properties at high pressure and temperature exists in the Earth's core maybe a compromise between extreme views of the metallic phase and inconformity with the high cosmic abundance of oxygen [121]. From this information, the outer core is rich in iron oxides are proposed.

In view of the topography, the downward migrating magma rich in iron oxides is affected by diffusion, obstruction of the inner core, tangentially geostrophic flow and toroidal flow, so the fluid flows westward, which may causes the geomagnetic secular variation. Under low viscosity, the oxides and metals can vertically and horizontally flow easily, thus allowing mutual oxidation-reduction reactions to take place in the F-layer. The active light metals take oxygen from heavy metal oxides and are further oxidized into light metal oxides, and the heavy metal oxides are reduced to heavy metals and falling precipitation in the inner core. For example:



CaO, MgO, Al<sub>2</sub>O<sub>3</sub>, Cr<sub>2</sub>O<sub>3</sub> and MnO float in the F-layer, and Fe<sub>2</sub>O<sub>3</sub>, FeO and NiO become iron and nickel, which sink down to be the main component of the inner core. These oxidation-reduction reactions are exothermic processes that produce a great amount of heat. The reduced iron alloys with certain amounts of nickel settle down at the ICB. By far the most provocative mechanism, the F-layer should be maintained through the interaction of separated melting and solidifying regions distributed over the ICB [122]. In the F-layer, magma diffuses and absorbs a great amount of heat to rise to the CMB and condenses into solid rock as the beginning of the process of a large convection cell starts anew. The great amount of heats, produced from radioactive elements generated nuclear energy, chemical reaction heat in the F-layer and nuclear fission heat near the center of the Earth, become the power sources for the geo-dynamo of great convection cell (Figure 4). Therefore, the Earth's geomagnetic secular variations and the geodynamical processes operates from the F-layer of outer core.





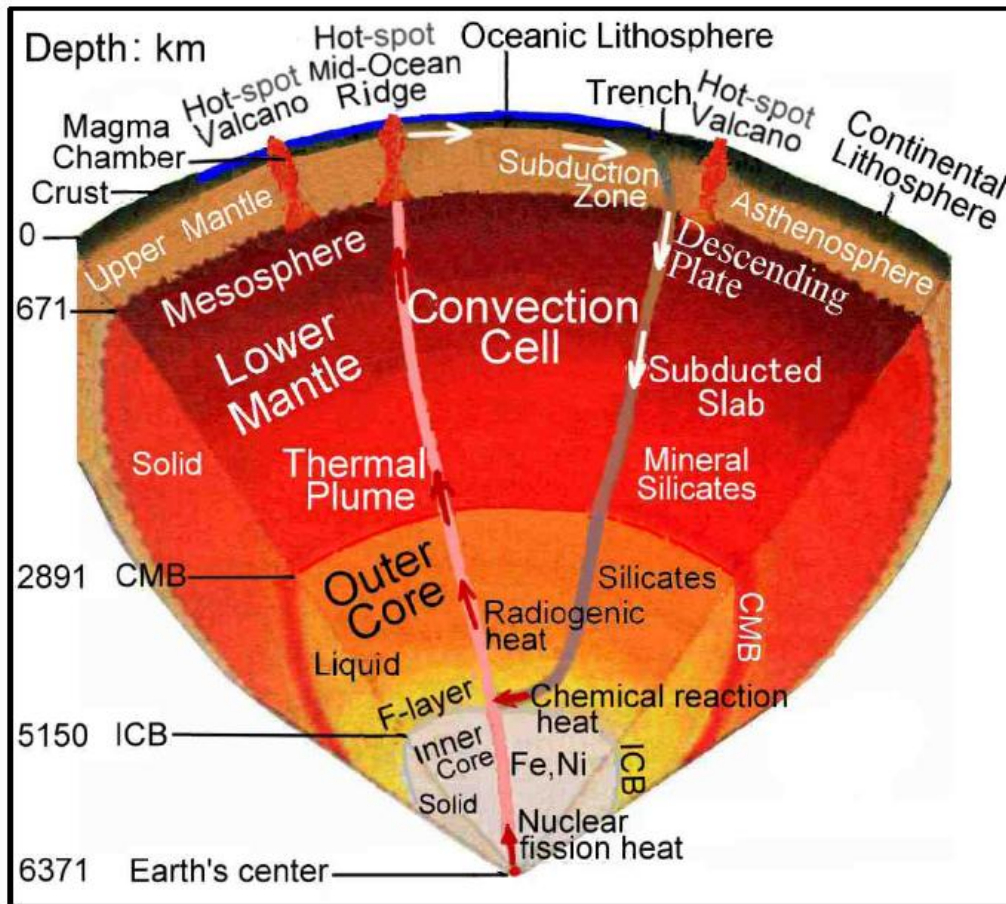


Figure 4: A schematic diagram of a great convection cell and heat flow, and the composition of Earth's interior

**Digital evaluation of the data in the new earth model**

In order to calculate the data of the Earth, the density distribution follows the divisions of the PREM divided into 94 levels, including 82 thin shells. The thickness of each shell is not greater than 100 km and so small compared with the Earth's radius of 6371 km that the density is regarded as linear variation within it. Then, a simplified method is applied to calculate the information of the Earth in order to simplify the calculating work.

The formula for the mass  $M$  of a uniform sphere can be derived through  $M = (4/3) \pi R^3 \rho$ . The mass  $\Delta M$  of each shell in the Earth's interior can be calculated through

$$\Delta M = (4/3)\pi\rho_t R_t^3 - (4/3)\pi\rho_b R_b^3 \tag{1}$$

Where  $\rho_t$ ,  $\rho_b$  are the densities at the top and the bottom, respectively, of one shell, and  $R_t$ ,  $R_b$  are the radii of the top and the bottom in a shell. Because the difference between  $R_t$  and  $R_b$  is so small and the density is regarded as linear variation in the shell, the mean value  $\bar{\rho}$  of both  $\rho_t$  and  $\rho_b$  is substituted for  $\rho_t$  and  $\rho_b$  in order to simplify the calculation. Then equation (1) becomes

$$\Delta M = (4/3)\pi\bar{\rho}(R_t^3 - R_b^3) \tag{2}$$

The moment of inertia of a sphere can be derived through  $I = CMR^2$ . Where  $C$  is the coefficient of the moment of inertia, which is  $2/5$  in a uniform sphere. The moment of inertia  $\Delta I$  of each shell in the Earth's interior can be calculated through

$$\Delta I = (8/15)\pi\bar{\rho}(R_t^5 - R_b^5) \tag{3}$$

From fluid mechanics, in a region of uniform composition, which is in a state of hydrostatic stress, the gradient of hydrostatic pressure is expressed by

$$dP/dR = -g\rho \tag{4}$$

Where  $P$ ,  $R$  are the pressure and the radius, respectively, at the region;  $\rho$  is the density at that depth;  $g$  is the acceleration due to gravity at the same depth.

If the effect of the Earth's rotation is negligible, the potential theory shows that  $g$  is resulted only from the attraction of the mass  $M$  within the sphere of radius  $R$  through

$$g = GM/R^2 \tag{5}$$

Where G is the gravitational constant  $6.6726 \times 10^{-11} \text{ m}^3/\text{kg} \cdot \text{s}^2$ .

Equation (5) substitutes into equation (4) and integrate it. In order to simplify the calculation,  $\rho$  and M are substituted by  $\bar{\rho}$  and  $\bar{m}$ , which are considered the constants in the thin shell and irrelative to the P and R. The result becomes

$$\Delta P = (1/R_b - 1/R_t)G\bar{m}\bar{\rho} \tag{6}$$

Where  $\Delta P$  is the difference in pressure between the top and the bottom in a layer of the Earth, and  $\bar{m}$  is the mass of a sphere as the mean value of the masses of the sphere within the top radius  $R_t$  and the bottom radius  $R_b$ , respectively, of a shell.

Equation (6) cannot be applied to the center of the Earth where is a discontinuous point. To integrate the portion of the center, the other form is applied as

$$\Delta P_c = (2/3)\pi G\bar{\rho}^2 R_c^2 \tag{7}$$

Where  $\Delta P_c$  is the difference in pressure between the radius  $R_c$  and the center of the Earth at the center portion.

The acceleration due to gravity  $g$  of each layer can be derived from equation (5). According to the observation data, the moment of inertia about the polar axis of the earth is  $0.3309 \text{ MeRe}^2$  and about an equatorial axis is  $0.3298 \text{ MeRe}^2$  [123]. The earth is regarded as a sphere, of which the moment of inertia is determined to be  $80286.4 \times 10^{40} \text{ g} \cdot \text{cm}^2$  by taking the mean value of both figures, where  $M_e$  is the earth's mass of  $5974.2 \times 10^{24} \text{ g}$  and  $R_e$  is the equatorial radius of 6378.14 km.

In order to examine the accuracy of applied equations, we apply the density distribution of the PREM to calculate the Earth's mass, moment of inertia, pressure and acceleration due to gravity in Table 1 (<http://newidea.org.tw/pdf/S60.pdf>). The calculated values of the earth's data from the density distribution of the Preliminary Reference Earth Mode as compared with the values of the current data and the PREM are listed in compared with that of the current data and the PREM are listed in Table 2.

**Table 2:** The calculated values of the simple method from the density distribution of the PREM as compared with the data of the PREM and the current earth

Data of the Earth	Mass	Moment of inertia	Pressure at CMB	Pressure at Earth center	Gravity at CMB	Gravity at Earth surface
Unit	$10^{24} \text{ g}$	$10^{40} \text{ g} \cdot \text{cm}^2$	kbar	kbar	$\text{cm}/\text{sec}^2$	$\text{cm}/\text{sec}^2$
PREM & Current	5972.200	80286.400	1357.509	3638.524	1068.230	981.560
Calculated values	5973.289	80205.664	1358.335	3655.973	1068.680	981.959
Difference %	-0.0152	-0.1006	+0.0608	+0.4796	+0.0421	+0.0406

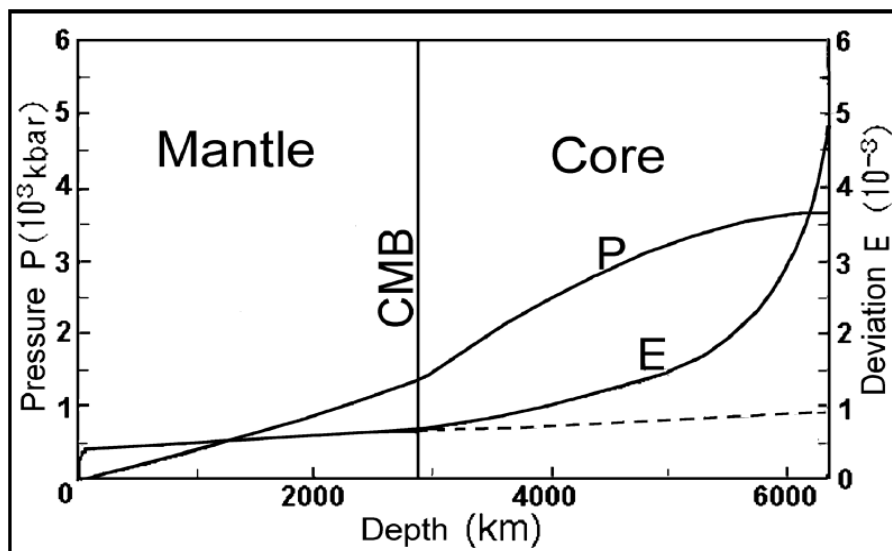


Figure 5: The pressure P of the PREM and the deviation E of the calculated pressure of simplified method from the value of P

From Table 2 the deviations of the calculated Earth's values from the data of the PREM and the current Earth are nearly within 0.1%, except the pressure at the Earth center. It indicates that the calculated values are very close to the current data and the simplified method is acceptable and useful; however, the calculated pressure of 3655.973 kbar at the Earth's center is higher than the data of the PREM of 3638.524 kbar by 0.4796 %, about 8 times of deviation at the CMB. We compare all the calculated pressures of the simplified method with that of the PREM by the curve of deviation E in Table 3 (<http://newidea.org.tw/pdf/S61.pdf>) and show the pressure P of the PREM in Figure 5. According to the Figure 5, the deviations E of Pressure curve from the crust to the CMB is showed nearly as a straight line, indicating that the calculated pressures have the systematic errors in view of the error theory. But from the CMB to the Earth's center, the slope of curve E sharply increases above the dashed line, which is the straight line extended from the CMB. It indicates that there is a considerable discrepancy within the core. We may suppose that the structure of the core in the PREM, which greatly affects its core pressure, is something wrong.

In order to investigate the structure of the Earth, particularly the core, four curves of density distribution are proposed to match the known conditions. From the crust to the CMB the curves of density distribution are adopted as the same of the PREM, and from the CMB to the ICB four plotted different curves are assumed. Due to a small jump of P-wave velocity at the boundary of F-layer in the outer core, the slope of density curve is nearly as steep as the PREM. There is a discontinuity at the ICB, so that a density jump of Derr's suggestion (2.0 g/cm<sup>3</sup>) is used [116]. In the inner core, the same slope of density curve of the PREM is used. The four density curves of the assumed Earth model compared with the PREM are shown in Figure 6.

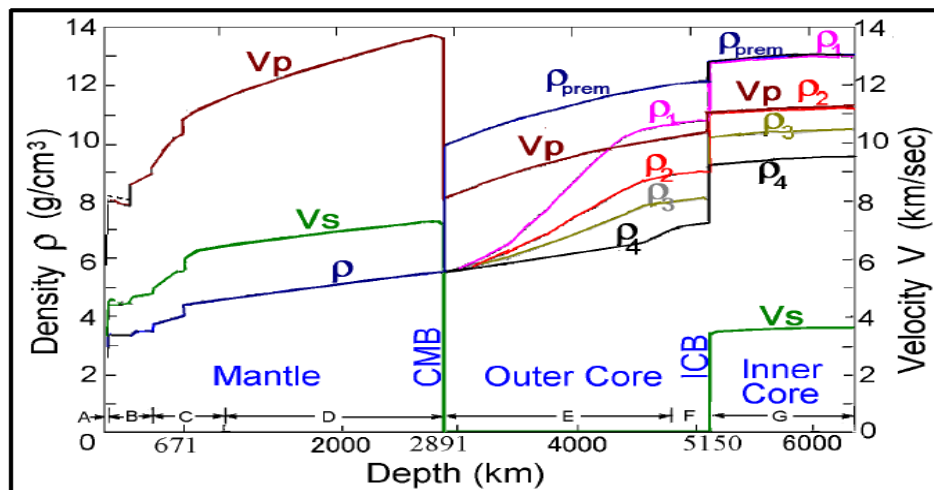


Figure 6: These densities  $\rho$  of the new Earth models 1, 2, 3 and 4 are compared with the PREM's.

The mass and the moment of inertia of four new Earth models can be determined, and compare with the current measured data of the Earth's mass of  $5974.2 \times 10^{24}$  g and moment of inertia of  $80286.4 \times 10^{40}$  g.cm<sup>2</sup>, then the differences will be found to be very large as Table 4 is shown. The differences are the insufficiencies of the mass and the moment of inertia of the four new Earth models.

Table 4: The insufficiencies of the mass and the moment of inertia in the four new earth models

Earth model	Unit	Observed value	New model 1	New model 2	New model 3	New model 4
Mass	$10^{24}$ g	5974.200	5409.024	5268.126	5204.761	5121.820
Insufficiency	$10^{24}$ g		565.176	706.074	769.439	852.380
Moment of inertia	$10^{40}$ g.cm <sup>2</sup>	80286.400	77007.472	76571.028	76378.768	76126.841
Insufficiency	$10^{40}$ g.cm <sup>2</sup>		3278.928	3715.372	3907.632	4159.559

The insufficiencies of the Earth's mass and moment of inertia, called the missing mass and moment of inertia, both are relative to the gravity that belong to the dark matter in astrophysics. It can only be obtained by comparing the observed data of the Earth, but cannot be detected directly and answered clearly through the ordinary Earth sciences. In order to solve the problems of the insufficiencies, a new study of the Earth is

attempted by utilizing the contemporary physics. If we can successfully explain that the insufficiencies exist in a suitable condition, a new Earth model will be established.

There are two types of dark matter: hot dark matter (HDM) and cold dark matter (CDM). Hot dark matter exists as such in a kind of photon or neutrino which has zero mass and moves at or approaching the speed of light. Cold dark matter exists at a lower energy and particle type. Due to the gravity of the particles, CDM moves at a low speed and collects together like normal matter. According to the observation data of background radiation in the universe, some physicists have recently proposed that perhaps cold dark matter explains the cosmic-structure. Blumenthal *et al* argued that the CDM model for the formation and distribution of galaxies in the universe is successful and the expansion of the universe is dominated by the CDM [124]. After reporting the South Pole experiment, Lubin *et al* showed that according to a recent anisotropy experiment in which a Bayesian analysis was used to constrain the amplitude of the perturbation spectrum, they showed that adiabatic HDM models were convincingly ruled out and CDM models had anisotropies near their derived limits [125]. Based on the result of their experiment, they announced the South Pole experiment was particularly well suited to the CDM-type model, among others.

Proceeding with the assumption, the missing mass and moment of inertia of the Earth are those of the CDM, which may constitute a normal planet. In order to find some solution in this article, the dark matter is compared to Mars. The average radius of Mars is 3397 km, and the mass  $642.40 \times 10^{24}$  g. In 1989, Kaula *et al* studied the moment of inertia of Mars and got the maximum allowable mean value is  $0.3650 MR^2$ , i.e.  $2689.8 \times 10^{40}$  g.cm<sup>2</sup> [126]. The insufficient data of 4 new Earth models roughly approach to the Mars', So, the dark matter is considered as a planet, called a dark planet, of which the form is similar to Mars and its characteristics are based on the inner planets of the solar system. In order to cut a figure of the dark planet, it is considered as a sphere, whose radius and density can be calculated from the insufficiencies of the Earth's mass and moment of inertia through the simplified method. The data of the dark planet can be calculated as following.

Considering the density of rock on the surface of the Earth and the Moon, the surface density  $2.70$  g/cm<sup>3</sup> of the dark planet is proposed. Under the condition that the density of a layer is proportional to its depth, a trial value of density at the center of the dark planet is selected, and applying the equations (2) and (3) to calculate the mass and the moment of inertia of each shell, the total mass and moment of inertia of it should be gotten. Because the radius and the center density of the dark planet are the hypothetical values, but the total mass and moment of inertia are necessary to correspond to the insufficiencies of the Earth's; therefore, it is necessary to use a trial-and-error approach to determine the proper radius and the center density.

Since the Earth's orbit around the Sun may be affected by the gravity of the dark planet, but no abnormal effect on the Earth has been observed. An assumption is suggested that the gravity centers of the Earth and the dark planet coincide with each other at the same point. It is inferred from the phenomenon in which the same side of the Moon always faces the Earth that means the Earth and the dark planet may rotate synchronously.

Assuming that the gravity centers of the Earth and the dark planet coincide at a single point and both rotate synchronously, the total values of mass and moment of inertia may be obtained from the sum of them. Based on mechanics, the gravity at each shell inside the Earth is affected by the mass of the Earth and the dark planet within its radius. The pressure difference  $\Delta P'$  between the top and the bottom of a shell within the Earth is calculated through

$$\Delta P' = (1/R_b - 1/R_t) G \bar{M}' \bar{\rho} \quad (8)$$

Where  $\bar{M}'$  is the mean value of the total mass of the Earth and the dark planet within the radius  $R_t$  and  $R_b$ .

Equation (8) cannot be applied to the Earth's center. The average density  $\bar{\rho}'$  of the central portion combined with the Earth and the dark planet within the radius  $R_c$  can be calculated through

$$\bar{\rho}' = (M_c + M_d) / [(4/3)\pi R_c^3] \quad (9)$$

Where  $M_c$  and  $M_d$  are the masses of central portion in the Earth and in the dark planet, respectively.

The difference of pressure  $\Delta P'_c$  between the top and the center of the central portion in the Earth can be obtained through

$$\Delta P'_c = (2/3)\pi G \bar{\rho} \bar{\rho}' R_c^2 \quad (10)$$

Based on the characteristics of the inner planets of the solar system except Mercury, the bigger the radius of a planet, the higher the average density is. So, the radius and the average density of a suitable dark planet must be





compatible with the characteristics of inner planet in solar system. The data of the four new Earth models and each dark planet are compared with the data of the current Earth and the PREM in the Table 5.

**Table 5:** The calculated data of the new four earth models compared with the data of the current earth and the PREM

Kind of Earth's model	The Earth planet								The darkplanet					
	Radius	Average density	Mass	Moment of inertia	Center density	Center pressure	Moment of inertia	Radius	Average density	Mass	Moment of inertia	Moment of inertia	Suitability	
Unit	km	g/cm <sup>3</sup>	10 <sup>24</sup> g	10 <sup>40</sup> gcm <sup>2</sup>	g/cm <sup>3</sup>	kbar	C	km	g/cm <sup>3</sup>	10 <sup>24</sup> g	10 <sup>40</sup> gcm <sup>2</sup>	C		
PREM	6371	5.5150	5974.200	80286.400	13.08848	3638.524	0.3309							
Model1	6371	4.9945	5409.024	77007.472	13.08848	3283.754	0.3508	3808.414	2.4427	565.176	3278.928	0.4000	no	
Model2	6371	4.8635	5268.126	76571.028	11.29785	3039.584	0.3581	3732.304	3.2421	706.074	3715.372	0.3777	no	
Model3	6371	4.8050	5204.761	76378.768	10.46002	2934.587	0.3615	3717.755	3.5747	769.439	3907.632	0.3674	no	
Model4	6371	4.7284	5121.820	76126.841	9.49821	2805.297	0.3662	3700.375	4.0161	852.380	4159.559	0.3564	good	

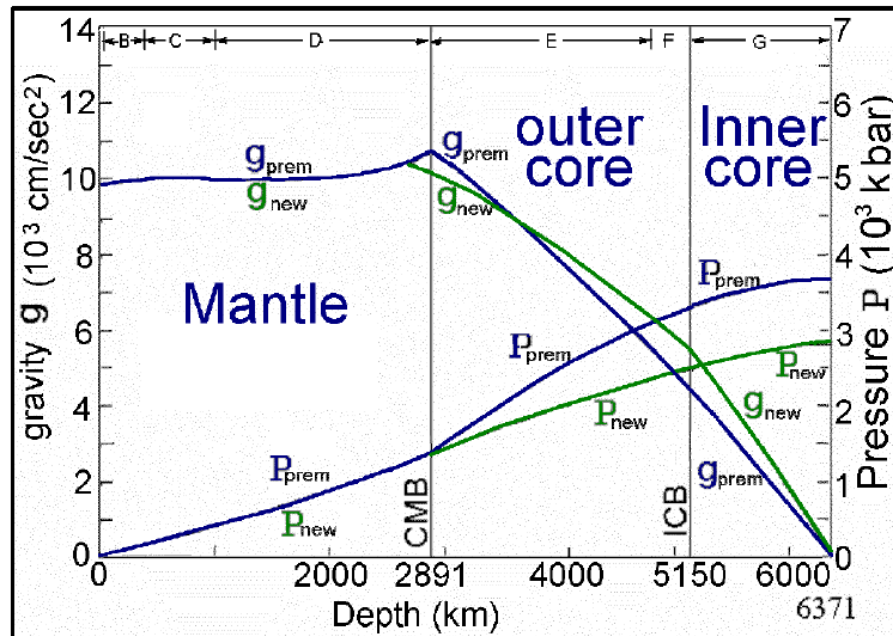


Figure 7: Diagram of the gravity  $g$  and the pressure  $P$  of the new Earth model and the PREM

The average radius of Mars is 3397 km, the mass  $642.40 \times 10^{24}$  g, and the average density  $3.912 \text{ g/cm}^3$ . Both values of the radius and the average density of the dark planet in the new Earth model 4 are bigger than those of Mars, therefore, this model is found to be the more suitable one.

The precise data of the Earth and the dark planet are calculated from the density distribution of the new Earth model 4, the data of the Earth planet is listed in Tables 6 (<http://newidea.org.tw/pdf/S62.pdf>), the dark planet is listed in Table 7 (<http://newidea.org.tw/pdf/S63.pdf>) and the global data of the new Earth model in Table 8 (<http://newidea.org.tw/pdf/S64.pdf>). The pressure  $P$  and the acceleration due to gravity  $g$  of the new Earth model compared with the PREM are shown in Figure 7. In this suitable model the slope of density curve from a depth about 400 km of the upper mantle through zones C, D and E to the upper boundary of F-layer is nearly a straight line, which means the density increase in proportion to its depth in accord with general physical phenomenon. So, the new Earth model 4 is acceptable as the proper new Earth model. We can find the pressure curve of the new Earth model is smoother than that of the PREM below the CMB. In the gravity curve of the



new Earth model, there are two deflection points in the curve that the one is at 2670.625 km in depth at the radius of the dark planet, and the other is at the ICB. The Earth has a mass of  $5121.820 \times 10^{24}$  g, a moment of inertia of  $76126.841 \times 10^{40}$  g.cm<sup>2</sup>, an average density of 4.7284 g/cm<sup>3</sup>. The Earth's center has a density of 9.49821 g/cm<sup>3</sup> and the pressure of 2805.297 kbar. The reduced values of the Earth's data from those of the current Earth are due to the existence of the dark planet. The dark planet has a radius of 3700.375 km, a moment of inertia of  $4159.559 \times 10^{40}$  g.cm<sup>2</sup>, an average density of 4.0161 g/cm<sup>3</sup> and a mass of  $852.380 \times 10^{24}$  g about 1.33 times of Mars. The data of the new Earth model compared with those of the current Earth and the PREM are listed in Table 10.

**Table 9.** The data of the new Earth model compared with the current Earth and the PREM

Data of planet	Radius	Mass	Inertia of moment	Average density	Center density	Center pressure	Coef-ficient
Unit	km	$10^{24}$ g	$10^{40}$ g.cm <sup>2</sup>	g/cm <sup>3</sup>	g/cm <sup>3</sup>	kbar	C
PREM and current earth	6371.000	5974.200	80286.400	5.515	13.08848	3638.524	0.3309
Earth planet	6371.000	5121.820	76126.841	4.7284	9.49821	2805.297	0.3662
Dark planet	3700.375	852.380	4159.559	4.0161	7.96097	1115.272	0.3564

The density of the Earth's center is 9.49821 g/cm<sup>3</sup>, which is much lower than 13.08848 g/cm<sup>3</sup> of the PREM. Its pressure is 2805.297 kbar, which is also much lower than 3638.524 kbar of the PREM. The composition of the inner core is generally believed to be dominantly iron with a small amount of alloyed nickel. From the pressure-density Hugoniot data, the density of iron under 2805.297 kbar of pressure is about 12.7 g/cm<sup>3</sup> [127], which is much greater than that of the new Earth model by 25%. The inner core is not pure iron but contains a significant fraction of light components [128, 129], and that explains why the density of the inner core is so much smaller than the current value. Therefore, an inference that the composition of the inner core is dominantly iron, alloyed with a small amount of nickel and also combined with a significant amount of oxides is suggested.

## Results and Discussion

Based on the new try, a study in a different view of the core, a great convection cell is developed, a circulation of magma and solid or molten rock migrating up to the crust and down across the CMB to the lowermost F-layer of outer core, causes the topography of the CMB, and from the core brings some matter as the metal platinum have come all the way to the surface of the Earth. This study introduces a new Earth model which should solve some inexplicable problems of the Earth science, such as the density jump, the core-mantle chemical equilibrium, the geomagnetic secular variation and the Chandler wobble. The anomalous properties of the CMB and the ICB should be apparently brightened after this study.

From the simplified method of evaluating the data of the new Earth model, compares with the current observed data of the Earth, there are 14.27 % of the mass and 5.18 % of the moment of inertia missing. From the conceptions of the String theory, a dark planet inside the Earth, whose mass and moment of inertia supply the missing portions of the current Earth, is virtuously developed. String theory has been pointed out by critics that the model has shortcomings and potential theoretical problems [130]. Among those problems, the most fundamental one is that geometric formulation of the model has not been well understood yet. If the geometry underlying the String theory has been determined that may give us the key insight into the model and will allow us to make definite predictions with the String theory.

From 10-dimensional space-time of the String theory develops a multiverse, which are three-cosmic framework of the Universes. After studying the existence of the dark planet in the Earth's interior, the three-cosmic framework of the Universes may be able to be confirmed. This result may be served as an indirect proof of the existence of the dark matter, which locates in the interior of the Earth but other space than ours. According to this framework there are triple Universes in the whole spaces, namely 1<sup>st</sup> Universe, 2<sup>nd</sup> Universe and 3<sup>rd</sup> Universe. The three-cosmic framework of U1, U2, and U3 have no relationship between any two Universes. In there no interacting force of nature exists, except gravitation force that is the characteristic of the dark matter. So, the dark planet, which is found through the gravity, may be in invisible space other than our Universe.

Scientists assume existence of "dark energy", which will cause the stars of the Universe expanding at an accelerating rate. But what dark energy is now the public knows nothing and unable to search. Since dark



energy, by convention, does not count as "matter", from data gathered by the Planck spacecraft, this is  $26.8 / (4.9 + 26.8) = 84.5$  (%). We can only detect the whole Universe 15.5 % normal matter, but 84.5 % dark matter, which may be the star's mass in other Universes than ours.

Cosmologists studying a map of the universe from data gathered by the Planck spacecraft, the map shows a stronger concentration in the south half of the sky and a 'cold spot' that cannot be explained by current understanding of physics. In 2005, Dr. Laura Mersini-Houghton, theoretical physicist at the University of North Carolina, and Professor Richard Holman, professor at Carnegie Mellon University, predicted that anomalies in radiation existed and the phenomenon can only have been caused by the pull of gravitational force from other Universes [15]. Because of containing the great quantity of stars 84.5 % in the other Universes, its mass are pulling the stars of our Universe accelerating expansion by gravity. Scientists interpret it is the effect of dark energy to cause, in fact, there is only a great amounts of dark matter in our Universe, but no dark energy. The cold spot may be the first 'hard evidence' that other universes exist has been found by scientists.

It is hard to examine the existence of the dark planet directly; however, that can be recognized from Chandler wobble. Referring to the orientation of the rotation axis of the Earth in space in addition to both precession and nutation, there is a wobble on the instantaneous axis of rotation of the Earth itself. The wobble alters the position of a point on the Earth relative to the pole of rotation. In 1891, Chandler pointed out that there are two different kinds of the wobble periods. One is a period of 12 months and the other is a period of 433 days, about 14 months. The former, called annual wobble, is obviously affected by the seasonal climate. The latter, called Chandler wobble, has not been solved the problem for more than one hundred years. The Chandler wobble is a small deviation that amounts to change of about 9 meters (30 ft.) at the point in the surface of the rotation axis of the Earth [131].

In 2000, Gross found that two-thirds of the Chandler wobble was caused by fluctuating pressure on the seabed, which, in turn, is caused by changes in the circulation of the oceans caused by variations in temperature, salinity and wind. The remaining third is due to atmospheric fluctuations [132]. The full explanation for the period also involves the fluid nature of the Earth's core and oceans. The wobble, in fact, produces a very small ocean tide with an amplitude of approximately 6 mm, called a "pole tide", which is the only tide not caused by an extraterrestrial body. While it has to be maintained by changes in the mass distribution or angular momentum of the Earth's outer core, atmosphere, oceans, or crust (from earthquakes), for a long time the actual source was unclear, since no available motions seemed to be coherent with what was driving the wobble.

Since that both the Earth and the dark planet spin synchronously around the same gravity center are postulated, but the rotation axes of both are impossible coinciding with each other. In other words, an angle between the two rotation axes produces the Chandler wobble as the precession and nutation due to the effects of the Sun and the Moon on non-parallel rotation axes with the Earth's. Therefore, the effect of Chandler wobble may confirm the existence of a dark planet inside the Earth.

From this study, the hypothesis of the three-cosmic framework of the Universes maybe enable a new way to find out about the abundant dark matter and solve some problems in astrophysics, such as:

1. Cygnus X-1 is a hot super giant star orbited by an invisible compact object in a period of 5.6 days [133]. The mass of the compact object can be estimated from the Doppler shifts in the spectrum of the visible super giant star. Its mass is about 9 times of the sun. This is considerably more than the maximum mass of a neutron star. Therefore, the compact object is not a neutron star or a white dwarf star. Since it has problems of optical confirmation, it is believed that the compact object may not be a black hole. If we consider the compact object of Cygnus X-1 as the dark matter in the other Universe than ours and its gravity affects Cygnus X-1, the problem may be solved.

2. Stars that evaporate from the Hyades cluster will remain within a few hundred parsecs (1 parsec = 3.26 light year) of the cluster only if they are dynamically bound to a much more massive entity containing the cluster. A local mass enhancement of at least  $(5-10) \times 10^5$  solar masses, with a radius of about 100 pc, can trap stars with an origin related to that of the Hyades cluster and explains the excess of stars with velocities near the Hyades velocity that constitutes the Hyades supercluster. Part of this mass enhancement can be in visible stars, but a substantial fraction is likely to be in the form of dark matter [134]. This dark matter should be in another Universe than ours.



3. Historically, the prediction of Halley's Comet has always been errors of 3 or 4 days in the predicted time of the perihelion passage. Joseph Brady, the scientist of California Institute of Technology, based on studies of periods of Halley's Comet using old European and Chinese records, and used a computer to treat the data of it in a numerical model of the solar system, he has been able to predict an invisible X planet (trans-plutonian planet), which was about three times the size of Saturn with highly inclined orbit ( $i=120^\circ$ ,  $e= \pm 0.07$ ) to the ecliptic and the time period of it to be 450 years [135,136]. Flandern proposed a search for an Xplanet, which has about three times the mass of the Earth and a highly inclined eccentric orbit that accounted for all of the perturbations on the motions of Neptune [137]. In 1988, NASA research scientist Anderson, presented the deviation of Neptune and Uranus in the regular orbit and proposed "The Theory of X Planet" from observed astronomical data of the nineteenth century. The mass of X planet is about five times that of the Earth and its period is about 700~1000 years. The orbit is elliptical and the inclination from the orbit to ecliptics very large and almost perpendicular [138]. Now the planet X has been searched for, but it still remains to be found. If the dark planet X orbits around the Sun in the other Universe than ours, then its gravity will sometimes affect the motion of Halley's Comet, Neptune and Uranus. Therefore, the problem of the invisible planet X may be solved.

This is absolutely a new try to break the bottlenecks of the research in the deep interior of the Earth in the geophysics and in the spaces of the Universe in the astrophysics. From the applications of the ten-dimensional space-time of String theory, the three-cosmic framework of the Universes is inferred. Some scientific problems of the geophysics and astrophysics, such as density jump, convection cell, composition of the Earth, dark matter, dark energy and multiverse, may be roughly solved as above, but that still needs to be proved by the fine outcomes of physicists' research.

#### Acknowledgement

I am grateful to Dr. Lin-Gun Liu of Research School of Earth Science in Australian for constructive criticisms and helpful comments in 1990.

#### References

- [1]. Zwicky, F. (1937). On the Masses of Nebulae and of Clusters of Nebulae. *Astrophysical Journal*, 86: 217.
- [2]. Bartusiak, Marcia, (1988). Wanted: Dark Matter, *Discover*, Dec., 63-69.
- [3]. Strobinskii A.A. & Zel'dovich, Ya. B. (1988). Quantum Effects in Cosmology, *Nature*, 331: 25.
- [4]. Riess Adam G. *et al.*, (High-z Supernova Search Team) (1998). Observational Evidence from Supernovae for an Accelerating Universe and a Cosmological Constant. *Astronomical Journal*, 116(3): 1009-1038.
- [5]. Perlmutter, S.; Aldering; Goldhaber; Knop; Nugent; Castro; Deustua; Fabbro; Goobar; Groom; Hook; Kim; Kim; Lee; Nunes; Pain; Pennypacker; Quimby; Lidman; Ellis; Irwin; McMahon; Ruiz-Lapuente; Walton; Schaefer; Boyle; Filippenko; Matheson; Fruchter; et al., (1999). Measurements of Omega and Lambda from 42 high redshift supernovae. *Astrophysical Journal*, 517(2): 565-86.
- [6]. Bennett, C.L. *et al.*, (2013). Nine-year Wilkinson Microwave Anisotropy Probe (WMAP) Observations: Final Maps and Result. *The Astrophysical Journal Supplement*, 208(2): 20.
- [7]. Ade, P.A.R., Aghanim, N., Armitage-Caplan, C. et al. (Planck Collaboration). (2014). Planck 2013 results. I. Overview of products and scientific results, *Astronomy & Astrophysics*, 5 Jun.
- [8]. Sawangwit, U. & Shanks, T. (2010). Durham astronomers' doubts about the 'dark side', *Royal Astronomical Society NEWS & PRESS*, 15. June.
- [9]. Schwarz, J.H. & Scherk, J. (1974). Dual models for non-hadrons. *Nuclear Physics*, B, 81: 118-144.
- [10]. Witten, Edward, (1995). String theory dynamics in various dimensions, *Nuclear Physics*, B. 443: 85.
- [11]. Witten, Edward, (1998). Magic, Mystery and Matrix, *Notices of the AMS*, October, 1124-1129.
- [12]. Scherk, J. & Schwarz, J.H. (1975). Dual field theory of quarks and gluons, *Physics Letters*, B, 57:463-466.
- [13]. Siegfried, T. (1999). Hidden Space Dimensions May Permit Parallel Universes, Explain Cosmic Mysteries. *The Dallas Morning News*, 5 July.



- [14]. Dvali, Georgi, (2004). Out of the Darkness, *Scientific American*, February, 68-75.
- [15]. Woit, Peter, (2013). The "Dark Flow" & Existence of Other Universes—New Claims of Hard Evidence, *New Scientist*, 3, June.
- [16]. Everett, Hugh, (1957). Relative State Formulation of Quantum Mechanics. *Reviews of Modern Physics*. 29: 454-462.
- [17]. Byrne, Peter, (2008). The Many Worlds of Hugh Everett, *Scientific American*, on October 21.
- [18]. Creager, K.C. & Jordan, T.H. (1986). A spherical structure of the core-mantle boundary from PKP travel time, *Geophysics. Res. Lett.*, 13: 1497-1500.
- [19]. Morelli, A. & Dziewonski, M. (1987). Topography of the core-mantle boundary and lateral homogeneity of the liquid core, *Nature*, 19, Feb., 325: 678-683.
- [20]. Jeanloz, R. (1990). The Nature of the Earth's Core, *Annual Review of Earth and Planetary Sciences*, 18: 357-386.
- [21]. Dziewonski, A.M. & Anderson, D.L., 1981. Preliminary Reference Earth Model, *Phys. Earth Planet. Inter.*, 25, 297-356.
- [22]. Ramsey, W.H. (1948). On the constitution of the terrestrial planets, *Mon. Not. Roy. Astron. Soc.*, 108: 406-413.
- [23]. Lyttleton, R.A. (1973). The end of the iron-core age, *Moon*, 7: 422-439.
- [24]. Knopoff, F. (1965). A preeminent seismology, *Phys. Rev.*, 138(A): 1445.
- [25]. Buchbinder, G.G.R. (1968). Properties of the Core-Mantle Boundary and Observations of PcP, *J. Geophys. Res.*, 73: 5901.
- [26]. Birch, Francis, (1939). The variation of seismic velocities within a simplified earth model in accordance with the theory of finite strain, *Bull. Seismol. Soc. Amer.*, 29: 463-479.
- [27]. Liu, Lin-Gun, (1974). Birch's Diagram; some new observations, *Phys. Earth Planet. Inter.*, 8: 56-62.
- [28]. Agnew, D., Berger, J., Buland, R., Farrell, W. & Gilbert, F. (1976). International Deployment of Accelerometers: a network for very long period seismology, *EOS, Trans. Am. Geophys. Union*, 57: 180-188.
- [29]. Peterson, J., Butler, H.M., Holcomb, L.G. & Hutt, C.R. (1976). The seismic research observatory, *Bull. Seism. Soc. Am.* 66: 2049-2068.
- [30]. Doornbos, D.J. & Hilton, T. (1989). Models of the core-mantle boundary and the travel times of internally reflected core phases, *J. Geophys. Res.*, 94(B11): 15,741-15,751.
- [31]. Forte, A.M. & Peltier, R.W. (1991). Mantle convection and core-mantle boundary topography: Explanations and implications, *Tectonophysics*, 187(1-3): 91-116.
- [32]. Neuberg, J. & Wahr, J. (1991). Detailed investigation of a spot on the core mantle boundary using digital PcP data, *Phys. Earth planet. Inter.*, 68: 132-143.
- [33]. Rodgers, A. & Wahr, J. (1993). Inference of core-mantle boundary topography from ISC PcP and PKP travel times. *Geophys. J. Int.* 115: 991-1011.
- [34]. Obayashi, M. & Fukao, Y. (1997). P and PcP travel time tomography for the core-mantle Boundary. *J. Geophys. Res.*, 102: 17825-17841.
- [35]. Boschi, L. & Dziewonski, A.M. (1999). High and low resolution images of the Earth's mantle: Implications of different approaches to tomographic modeling, *J. Geophys. Res.*, 104 (B11): 25567-25594.
- [36]. Boschi, L. & Dziewonski, A.M. (2000). Whole Earth tomography from delay times of P, PcP, and PKP phases lateral heterogeneities in the outer core or radial anisotropy in the mantle? *J. Geophys. Res.*, 105: 13675-13696.
- [37]. Garcia, R. & Souriau, A. (2000). Amplitude of the core-mantle boundary topography estimated by stochastic analysis of core phases. *Phys. Earth Planet. Inter.*, 117: 345-359.
- [38]. Sze, E.K.M. & van der Hilst, R.D. (2003). Core mantle boundary topography from short period PcP, PKP and PKKP data, *Physics of the Earth and Planetary Interiors*, 135: 27-46.
- [39]. Yoshida, M. (2008). Core-mantle boundary topography estimated from numerical simulations of instantaneous flow. *Geochem. Geophys. Geosys.* 9(7).



- [40]. Soldati, G., Koelemeijer, P., Boschi, L. & Deuss A. (2013). Constraints on core-mantle boundary topography from normal mode splitting, *Geochem. Geophys. Geosys.* 14.
- [41]. Soldati, G., Boschi, L., Mora, S.D. & Forte, A.M. (2014). Tomography of core-mantle boundary and lowermost mantle coupled by geodynamics: joint models of shear and compressional velocity, *Annals of Geophysics*, 6: 57.
- [42]. Woodhouse, J.H. & Dziewonski, A.M. (1989). Seismic modeling of the Earth's large-scale three-dimensional structure, *Phil. Trans. R. Soc. Lond.* A 328, 291-308.
- [43]. Engdahl, E.R., van der Hilst, R. & Buland, R. (1998). Global teleseismic earthquake relocation with improved travel time and procedures for depth determination. *Bull. Seism. Soc. Am.* 88: 722-743.
- [44]. Koelemeijer, P.J., Deuss, A. & Trampert J. (2012). Normal mode sensitivity to Earth's D" layer and topography on the core-mantle boundary: what we can and cannot see. *Geophys. J. Int.*, 190: 553-568.
- [45]. Bloxham, J. & Gubbins, D. (1987). Thermal core-mantle interactions. *Nature*, 325: 511-513.
- [46]. Stevenson, D.J. (1987). Limits on lateral density and velocity variations in the Earth's outer core, *Geophysics. J. R. Astr. Soc.*, 88: 311-319.
- [47]. Young, C.J. & Lay, T. (1987). The core-mantle boundary, *Ann. Rev. Earth Planet. Sci.*, 15: 25-46.
- [48]. Ruff, L. & Anderson, D.L. (1980). Core formation, evolution, and convection: A geophysical model, *Phys. Earth Planet. Inter.*, 21: 181-201.
- [49]. Bloxham, J. & Jackson, A. (1990). Lateral temperature variations at the core-mantle boundary deduced from the magnetic field, *Physical Review Letters*, 17(11): 1997-2000.
- [50]. Lay, T. (1989). Structure of the Core-Mantle Transition Zone: A Chemical and Thermal Boundary Layer, *EOS*, Jan., 70(4): 24, 49, 54-55, 58-59.
- [51]. Gubbins, D. & Richards, M.A. (1986). Coupling of the core dynamo and mantle: Thermal or Topography? *Physical Review Letters*, 13: 1521-1524.
- [52]. Morgan, W.J. (1971). Convection plumes in the lower mantle: *Nature*, 230: 42-43.
- [53]. Morgan, W.J. (1972). Deep mantle convection plumes and plate motions, *Bull. Am. Assoc. Pet. Geol.*, 56: 203-213.
- [54]. Hand, E. (2015). Mantle plumes seen rising from Earth's core, *Science*, 349(6252): 1032-1033.
- [55]. Puchkov, V.N. (2009). The Controversy over Plumes: Who Is Actually Right? *Geotectonics*, 43(1): 1-17.
- [56]. Van Schmus, W.R. (1995). Natural radioactivity of the crust and mantle, *Global Earth Physics: A Handbook of Physical Constants*, 283-291.
- [57]. Kerr, Richard A. (1997). Deep-Sinking Slabs Stir the Mantle. *Science*, AAAS. Retrieved 2013-06-13.
- [58]. Mjelde, R. & Faleide, J.I. (2009). Variation of Icelandic and Hawaiian magmatism: evidence for co-pulsation of mantle plumes? *Mar. Geophys. Res.*, 30: 61-72.
- [59]. Mjelde, R., Wessel, P. & Müller, D. (2010). Global pulsations of intraplate magmatism through the Cenozoic. *Lithosphere*, 2(5): 361-376.
- [60]. Pollack, H.N., Hurter, S.J. & Johnson, J.R. (1993). Heat flow from the Earth's interior: Analysis of the global data set, *Rev. Geophys.*, 31: 267-280.
- [61]. Jaupart, C., Labrosse, S. & Mareschal, J.C. (2007). Temperature, heat and energy in the mantle of the Earth, *Geophysics*, 7: 253-303.
- [62]. Lay, T., Hernlund, J. & Buffett, B.A. (2008). Core-mantle boundary heat flow. *Nature Geoscience*, 1(1): 25-32.
- [63]. Davies, J.H. & Davies, D.R. (2010). Earth's surface heat flux, *Solid Earth*, 1: 5-24.
- [64]. Davies, J.H. (2013). Global Surface Heat Flow Map, *Geophysical Research Abstracts*, 15: EGU2013-10885.
- [65]. Javoy, M. (1999). Chemical Earth models. *Comptes Rendus de l'Académie des Sciences Series II, A, Earth and Planetary Science*, 329: 537-555.
- [66]. Dye, S.T. (2012). Geoneutrinos and the radioactive power of the Earth, *Reviews of Geophysics*, 50(RG3007): 1-19.
- [67]. Fiorentini, G., Lissia, M. & Mantovani, F. (2007). Geo-neutrinos and Earth's interior, *Phys. Rep.*, 453: 117-172.





- [68]. Gando, A., Dwyer, D.A., McKeown, R.D., Zhang, C. (2011). Partial radiogenic heat model for Earth revealed by geoneutrino measurements, *Nat. Geosci.*, 4: 647-651.
- [69]. Araki, T. et al. (KamLAND Collaboration). (2005). Experimental investigation of geologically produced antineutrinos with KamLAND, *Nature*, 436: 499-503.
- [70]. Bellini, G. et al. (Borexino Collaboration), (2010). Observation of geo-neutrinos, *Phys. Lett. B*, 687(4-5): 299-304.
- [71]. Kuroda, P.K. (1956). On the Nuclear Physical Stability of the Uranium Minerals. *Journal of Chemical Physics*, 25 (4): 781-782; 1295-1296.
- [72]. Fermi, E. (1947). Nuclear reactor theory, *Science*, 105: 27-32.
- [73]. Hagemann, R. & Roth, E. (1978). Relevance of the studies of the Oklo natural reactors to the storage of radioactive wastes. *Radiochemica Acta*, 25: 241-247.
- [74]. Meshik, A.P., Hohenberg, C.M. & Pravdivtseva, O.V. (2004). Record of cycling operation of the natural nuclear reactor in the Oklo/Okelobondo area in Gabon. *Phys. Rev. Lett.*, 93: 182302.
- [75]. Hollenbach, D.F. & Herndon, J.M. (2001). Deep-earth reactor: nuclear fission, helium, and the geomagnetic field. *Proc. Nat. Acad. Sci. USA*, 98(20): 11085-11090.
- [76]. Gubbins, D. & Masters, T.G. (1979). *Adv. Geophys.* 59: 57-99.
- [77]. Korenaga, J. (2008). Urey ratio and the structure and evolution of Earth's mantle, *Reviews of Geophysics*, June, 2: 46.
- [78]. Hecht, J. (1995). Buried treasure from hot heart of the Earth, *New Scientist*, 19: 16.
- [79]. Basu A.R., Poreda R.J., Renne P.R., Teichmann F., Vasiliev Y.R., Sobolev N.V. & Turrin B.D. (1995). High <sup>3</sup>He plume origin and temporal-spatial evolution of the Siberian flood basalts, *Science*, 269: 822-825.
- [80]. Walker R.J. & Morgan J.W., Horan M.F. (1995). Osmium-187 in some plumes: Evidence for core-mantle interaction? *Science*, 269: 819-822.
- [81]. Knittle, E. & Jeanloz, R. (1991). The high-pressure phase diagram of Fe<sub>0.94</sub>O : A possible constituent of the Earth's core, *J. Geophysics. Res.*, 96: 16169-16180.
- [82]. Kubala, Bizy, & Mahan Rao, (1996). *Earth's Core Temperature*. Byrdand Black.
- [83]. Condie, Kent C. (1997). *Plate tectonics and crustal evolution* (4<sup>th</sup> Ed.). Butterworth-Heinemann, p. 5.
- [84]. Fiquet, G., Auzende, A.L., Siebert, J., Corgne, A., Bureau, H., Ozawa, H. & Garbarino, G. (2010). Melting of peridotite to 140 gigapascals. *Science*, 329: 1516-1518.
- [85]. Jeanloz, R. & Wenk, H.R. (1988). Convection and anisotropy of the inner core, *Geophysics. Res. Lett.* 15: 72-75.
- [86]. Singh, S.C., Taylor, M.A.J. & Montagner, J.P. (2000). On the presence of liquid in Earth's inner core. *Science*, 287: 2471-2474.
- [87]. Bergman, M.I. (2003). Solidification of the Earth's core, in Earth's Core: Dynamics, Structure, Rotation, *Geodyn. Ser.*, 105-127.
- [88]. Shimizu, H., Poirier, J.P. & Le Mouél, J.L. (2005). On crystallization at the inner core boundary. *Phys. Earth Planet. Inter.* 151: 37-51.
- [89]. Song, X. & Dai, W. (2008). Topography of Earth's inner core boundary from high-quality waveform, *Geophysical Journal International*, 175(1): 386-399.
- [90]. Waszek, L. & Deuss, A. (2015a). Observations of exotic inner core waves, *Geophys. J. Int.*, 200(3): 1636-1650.
- [91]. Pejić, T. & Tkalčić, H. (2016). Toward attenuation tomography of the uppermost inner core from PKP waves, *Geophysical Research Abstracts*, 18: EGU 2016-1605.
- [92]. Jeffreys, H. (1939). The times of the core waves, *Mon. Not. R. Astron. Soc. Geophys. Suppl.*, 4: 498.
- [93]. Bolt, Bruce A. (1972). The density distribution near the base of the mantle and near the Earth's center, *Phys. Earth Planet. Inter.*, 5: 301-311.
- [94]. Qamar, A. (1973). Revised velocities in the Earth's core, *Bull. Seismol. Soc. Am.*, 63: 1073- 1105.
- [95]. Cormier, V.F. (2009). A glassy lowermost outer core. *Geophys. J. Int.*, 179: 374-380.
- [96]. Souriau, A. & Poupinet, G. (1991). The velocity profile at the base of the liquid core from PKP (BC + Cdiff) data: An argument in favor of radial inhomogeneity, *Geophys. Res. Lett.*, 18: 2023-2026.



- [97]. Zou, Z., Koper, K.D. & Cormier, V.F. (2008). The structure of the base of the outer core inferred from seismic waves diffracted around the inner core, *J. Geophys. Res.*, 113: B05314.
- [98]. Cormier, V.F., Attanayake, J. & He, K. (2011). Inner core freezing and melting: constraints from seismic body waves. *Phys. Earth Planet. Inter.*, 188: 163-172.
- [99]. Rial, J.A. & Cormier, V.F. (1980). Seismic waves at the Epicenter's antipodes, *J. Geophys. Res.*, 91: 10203-10228.
- [100]. Cormier, V.F., 1981. Short-period PKP phases and the inelastic mechanism of the inner core, *Phys. Earth Planet. Inter.*, 24: 291-301.
- [101]. Choy, G.L. & Cormier, V.F. (1983). The structure of the inner core inferred from short-period and broad-band GDSN data, *Geophys. J. R. Astr. Soc.*, 72: 1-21.
- [102]. Song, X. & Helmberger, Don V. (1995). A P wave velocity model of earth's core, *J. Geophys. Res.*, 100(B7): 9817-9830.
- [103]. Kennett, B.L.N., Engdahl, E.R. & Buland, R. (1995). Constraints on seismic velocities in the Earth from travel times, *Geophys. J. Int.*, 122: 108- 124.
- [104]. Yu, W., Wen, L. & Niu, F. (2005). Seismic velocity structure in the Earth's outer core, *J. Geophys. Res.*, 110: B02302.
- [105]. Bullen, K.E. & Bolt, B.A. (1986). *An Introduction to the Theory of Seismology*, 4<sup>th</sup> Ed., Geophysical Journal of the Royal Astronomical Society, 86(1): 215-216.
- [106]. Sumita, I. & Olson, P. (1999). A laboratory model for convection in Earth's core driven by a thermally heterogeneous mantle. *Science*, 286: 1547-1549.
- [107]. Sumita, I. & Olson, P. (2002). Rotating thermal convection experiments in a hemispherical shell with heterogeneous boundary heat flux: implications for the Earth's core. *J. Geophys. Res.*, 107: 2169.
- [108]. Aubert, J., Amit, H., Hulot, G. & Olson, P. (2008). Thermochemical flows couple the Earth's inner core growth to mantle heterogeneity, *Nature*, 454: 758-762.
- [109]. Bolt, Bruce A. & Qamar, A. (1970). Upper bound to the density jump at the boundary of the Earth's inner core, *Nature*, 228: 148-150.
- [110]. Souriau, A. & Souriau, M. (1989). Ellipticity and density at the inner core boundary from subcritical PKiKP and PcP data, *Geophys. J. Int.*, 98: 39-54.
- [111]. Shearer, P. & Masters, G. (1990). The density and shear velocity contrast at the inner core boundary, *Geophys. J. Int.*, 102: 491-498.
- [112]. Waszek, L. & Deuss, A. (2015b). Anomalously strong observations of PKiKP/PcP amplitude ratios on a global scale, *J. Geophys. Res. Solid Earth*, 120.
- [113]. Jeanloz, R. & Ahrens, T.J. (1980). Equations of FeO and CaO, *Geophys. J. R. Astr. Soc.*, 62: 505-528.
- [114]. McQueen, R.G., Marsh, S.P., Taylor, J.W., Fritz, J.N. & Carter, W.J. (1970). *The equation of state of solids from shock wave studies, in high velocity impact phenomena*, Kinslow, R., Academic Press, New York, 294-419.
- [115]. Hall, T.H. & Murthy, V.R. (1972). Comments on the Chemical Structure of a Fe-Ni-S Core of the Earth, *EOS*. 53(5): 602.
- [116]. Derr, J.S. (1969). Internal Structure of the Earth Inferred from Free Oscillations, *J. Geophys. Res.*, 74: 5202-5220.
- [117]. McFadden, Phillip L. & Merrill Ronald T. (1995). History of Earth's magnetic field and possible connections to core-mantle boundary processes. *J. Geophys. Res.*, 100: 307-316.
- [118]. Dziewonski, A.M. & Woodhouse, J.H. (1987). Global Images of the Earth's Interior, *Science*, 236(4797): 37-48.
- [119]. Anzellini, S., Dewaele, A., Mezouar, M., Loubeyre, P. & Morard, G. (2013). Melting of Iron at Earth's Inner Core Boundary Based on Fast X-ray Diffraction, *Science*, 340 (6131): 464-466.
- [120]. Gubbins, D., Masters, T.G. & Nimmo, F. (2008). A thermochemical boundary layer at the base of Earth's outer core and independent estimate of core heat flux, *Geophys. J. Int.*, 174: 1007-1018.
- [121]. Altshuler, L.V. & Sharipdzhanov, L.V. (1971). On the distribution of iron in the Earth, the chemical distribution of the latter. *Bull. Acad. Sci. USSR, Geophys. Ser.* 4: 3-16.



- [122]. Alboussière, T., Deguen, R. & Melzani, M. (2010). Melting-induced stratification above the Earth's inner core due to convective translation. *Nature*, 466: 744-747.
- [123]. Garland, G. D. (1979). *Introduction to Geophysics*. W. B. Saunders Company, Toronto, Canada. 2<sup>nd</sup> ED., 4-8, 28-30, 44-46, 130, 387-389.
- [124]. Blumenthal, G.R., Faber, S.M., Primack, J.R. & Rees, M.J. (1984). Formation of galaxies and large-scale structure with cold dark matter. *Nature*, 311: 517-525.
- [125]. Lubin, P.M., Bond, J R., Efstathiou, G. & Meinhold, P.R. (1991). Cosmic-Structure Constraints from a One-Degree Microwave-Back-ground Anisotropy Experiment. *Physical Review Letters*, 66: 2179-2182.
- [126]. Kaula, W.M., Sleep, N.H. & Phillips, R.J. (1989). More about the Moment of Inertia of Mars, *Geophysical Research Letters*, 16(11): 1333-1336.
- [127]. Ahrens, T.J. (1980). Dynamic Compression of Earth Materials, *Science*, 207: 1035.
- [128]. Ringwood, A.E. (1984). The Earth's Core: its composition, formation and bearing upon the origin of the Earth, *Proc. R. Soc. A*, 395: 1-46.
- [129]. Jephcoat, A. & Olson, P. (1987). Is the Inner Core of the Earth Pure Iron? *Nature*, 325: 332-335.
- [130]. Kaku, M. (1988). *Introduction to Superstrings*, Springer Verlag New York Inc., New York, USA. 16-18.
- [131]. Chandler, S. C. (1891). On the variation of latitude, *Astronomical Journal*, 11:59-61, 65-70.
- [132]. Gross, Richard S. (2000). The Excitation of the Chandler Wobble, *Geophysical Research Letters*, 27(15): 2329-2332.
- [133]. Stokes, G.M. & Michalsky, J.J. (1979). Cygnus X-1, *Mercury*, 8: 60.
- [134]. Casertano, S., Iben, I. & Shields, A. (1993).The Hyades Cluster-Supercluster Connection: Evidence for a Local Concentration of Dark Matter, *Astrophysical Journal*, Part 1, 410: 90-98.
- [135]. Brady, Joseph L. (1971). The orbit of Halley's Comet and apparition of 1896, *Astronomical Journal*, 76(8): 728-739.
- [136]. Brady, Joseph L. (1972).The Effect of Trans-plutonian Planet on Halley's Comet. *Publication of the Astronomical Society of the Pacific*, 34(498): 314-322.
- [137]. Flandern, T.V. (1981). The renewal of the Trans-Neptunian planet search, *Bulletin of the American Astronomical Society*, 12: 830.
- [138]. Anderson, John, 1988. Planet X - Fact or Fiction? *Planetary Report*, 8 (4): 6-9.

